Meteoritics & Planetary Science 32, 929–944 (1997)

A magma ocean on Vesta: Core formation and petrogenesis of eucrites and diogenites

KEVIN RIGHTER* AND MICHAEL J. DRAKE

Lunar and Planetary Laboratory, University of Arizona, Tucson, Arizona 85721, USA
*Correspondence author's e-mail address: righter@lpl.arizona.edu

(Received 1997 January 13; accepted in revised form 1997 July 9)
(Presented at the Workshop on Vesta and the HED Meteorites, Houston, Texas, USA, 1996 October 16–18)

Abstract–Available evidence strongly suggests that the HED (howardite, eucrite, diogenite) meteorites are samples of asteroid 4 Vesta. Abundances of the moderately siderophile elements (Ni, Co, Mo, W and P) in the HED mantle indicate that the parent body may have been completely molten during its early history. During cooling of a chondritic composition magma ocean, equilibrium crystallization is fostered by the suspension of crystals in a convecting magma ocean until the crystal fraction reaches a critical value near 0.80, when the convective system freezes and melts segregate from crystals by gravitational forces. The extruded liquids are similar in composition to Main Group and Stannern trend eucrites, and the last pyroxenes to precipitate out of this ocean (before convective lockup) span the compositional range of the diogenites. Subsequent fractional crystallization of a Main Group eucrite liquid, which has been isolated as a body of magma, produces the Nuevo Laredo trend and the cumulate eucrites. The predicted cumulate mineral compositions are in close agreement with phase compositions analyzed in the cumulate eucrites. Thus, eucrites and diogenites are shown to have formed as part of a simple and continuous crystallization sequence starting with a magma ocean environment on an asteroidal size parent body that is consistent with Vesta.

INTRODUCTION

The howardite, eucrite and diogenite (HED) meteorites are igneous rocks comprising both cumulate and noncumulate types. Most eucrites are metamorphosed breccias; noncumulate eucrites are basaltic, a small number of eucrites are coarse-grained pyroxene-plagioclase cumulates, and diogenites are orthopyroxene cumulates. All noncumulate eucrites have crystallization ages 8–20 Ma younger than T_0 (defined as the age of refractory inclusions in the Allende CV3 chondrite; Nyquist *et al.*, 1986; Carlson *et al.*, 1988; Allegre *et al.*, 1995; Shukolyukov and Lugmair, 1997). Both eucritic and diogenitic lithologies are found together in the howardite meteorites (polymict breccias), which suggests that all three meteorite types are related and come from the same parent body (Takeda *et al.*, 1976); support for this idea is provided by O isotope analysis (Clayton and Mayeda, 1996). Early suggestions that asteroid 4 Vesta may be a source of eucritic material (McCord *et al.*, 1970; Consolmagno and Drake, 1977) have recently been strengthened by the findings of Binzel and Xu (1993). Throughout this paper, the term "HED parent body" will be used to refer to a Vesta size asteroid, if not Vesta.

Recovery and chemical analysis of close to 100 eucrites has resulted in the recognition of three different groups of these meteorites: the Main Group eucrites, the Stannern trend, and the Nuevo Laredo trend (*e.g.*, BVSP, 1981) and two distinct schools of thought regarding their origin. The first hypothesis is that all eucrites are the end result of a fractional crystallization sequence, the cumulates of which are represented by the diogenites and cumulate eucrites (*e.g.*, Mason, 1962; Ikeda and Takeda, 1985; Warren, 1985a; Delaney *et al.*, 1984; Bartels and Grove, 1991; Longhi and Pan, 1988). None of these models has been able to account for all of the compositional variation seen in either the liquids or the cumulates without appealing to several different melting or fractionation events, polybaric fractionation (Longhi and Pan, 1988), or localized heating within the mantle of the parent body (*e.g.*, Grove and Bartels, 1992).

The second hypothesis argues that Main Group and Stannern trend eucrites are the result of different degrees of equilibrium partial melting of chondritic material (Stolper, 1977; Consolmagno and Drake, 1977) and since then has been the focus of many studies (Jurewicz *et al.*, 1991, 1995; Jones *et al.*, 1996). Although this second hypothesis is consistent with the clustering of the eucrites around the olivine-pyroxene peritectic point on an olivine-pyroxene-plagioclase phase diagram, and calls on later fractional crystallization of Main Group eucritic liquid to produce the Nuevo Laredo trend, it fails to account for the diogenites in a simple petrogenetic model (Shearer *et al.*, 1993; Mittlefehldt, 1994) and for the low Na contents of the eucritic plagioclase and HED parent body (Mason, 1969).

Both of these general ideas for the formation of HED meteorites are difficult to reconcile with the timing and physical conditions required for core formation in asteroid size bodies. Core formation in asteroid size planetesimals occurred early (<15 Ma after T_0) as has been recently demonstrated by Lee and Halliday (1996, 1997) and Harper and Jacobsen (1995) using $^{182}W/^{184}W$ ratios. Depletion of siderophile elements in the mantle of the HED parent body has been cited as evidence that metal had segregated into a core before the eucrites formed (see *e.g.*, Hewins and Newsom, 1988). Calculations of Taylor (1992) indicate that large degrees of melting are required to efficiently separate metal from silicate. The need for large degrees of melting for efficient segregation of metal from silicate has been demonstrated in the chondrite melting experiments of Takahashi (1983), where metallic blebs were left stranded within a silicate melt-olivine matrix even with 30% silicate melt present. Given the depletions of siderophile elements, it seems necessary to have large amounts of melting on a Vesta size body in order to facilitate core formation.

The partial melting hypothesis would require the HED parent body to have completely melted to form the core, solidified to form the mantle, and then melted later, perhaps repeatedly to explain the array of basaltic and cumulate meteorites. The reliance of such scenarios on later heating events has always been problematic, since many of the heat sources available in the early solar system are short lived, such as decay of ^{26}Al ($T_{1/2}$ = 0.7 Ma) or ^{60}Fe ($T_{1/2}$ = 0.3 Ma), a hot T-Tauri or FU Orionis stage, or a superluminous sun.

We have demonstrated (Righter and Drake, 1996) that moderately siderophile elements (Ni, Co, Mo, W and P) in the HED parent planet are best reconciled with core segregation during extensive melting of that body. The high temperatures necessary to melt a chondritic mantle to produce a magma ocean could be provided early (2–5 Ma after T_0) by the decay of ^{26}Al to ^{26}Mg (*e.g.*, Miyamoto, 1991; Russell *et al.*, 1996) and ^{60}Fe to ^{60}Ni (Shukolyukov and Lugmair, 1993). Here, we examine the sensitivity of our conclusion to the choice of different possible chondritic bulk compositions. We find that the conclusion of extensive melting of the HED parent body is robust for a wide range of possible chondritic compositions.

We have also modeled the crystallization history of a cooling magma ocean using two different modelling programs: MELTS (Ghiorso and Sack, 1995) and MAGPOX/MAGFOX (Longhi, 1987; Longhi and Pan, 1988). We demonstrate, using both chemical and physical arguments, that Main Group eucrites and diogenites may have been generated as part of a simple equilibrium crystallization sequence during cooling of a chondritic magma ocean. Equilibrium crystallization is fostered by the suspension of crystals in a convecting magma ocean until the crystal fraction reaches a critical value near 0.80, when the convective system freezes and melts segregate from crystals due to gravitational forces. The extruded liquids and resulting cumulates are similar in composition to Main Group and Stannern trend eucrites, and diogenites, respectively.

This physical scenario is appealing in that it allows all of these meteorites to form as part of a simple crystallization sequence without requiring anomalous or late heating events, it is consistent with the physical processes known to be important during both metal-silicate separation and later convection in a magma ocean (*e.g.*, Taylor *et al.*, 1993), and with calculations of the depth of material derived by impact cratering and excavation of a layered, Vesta size body (Asphaug, 1996).

MODELING OF CORE FORMATION IN VESTA

The first quantitative attempts at modeling core formation in the HED parent body were based on Co, Mo and W abundances (Newsom and Drake, 1982; Newsom, 1985). These results indicated that the abundances of these elements and Ni were consistent with a metallic core comprising 40–50% of the mass of the asteroid and with ~50% partial melting of the silicate mantle. Newsom's inability to match P abundances was attributed to the volatile behavior of P and the alkalis in the HED parent body (see also Mittlefehldt, 1987). However, P and Mn have nearly the same volatility, and since Mn is not depleted in the HED parent body (it is present at nearly chondritic levels; Drake *et al.*, 1989), P may have been present in CI chondritic levels (Drake *et al.*, 1989).

Righter and Drake (1996) reexamined the issue of core formation in a CI chondritic HED parent body by considering siderophile element partitioning during metal-silicate equilibrium at high temperatures. Here, we extend this work to investigate the effect of bulk composition by considering CM, CO, CV, H , L, and LL chondritic starting materials.

Abundances of Moderately Siderophile Elements in the Howardite, Eucrite, Diogenite Parent Body Mantle

Estimating the abundances of the moderately siderophile elements Ni, Co, Mo, W and P in a planetary mantle from which we have only basaltic samples is a challenge, but much is learned from comparison with terrestrial mantle and basalt samples (*e.g.*, Delano, 1986). We will consider Ni and Co, which behave as compatible elements in olivine and orthopyroxene, and Mo, W and P, which are incompatible

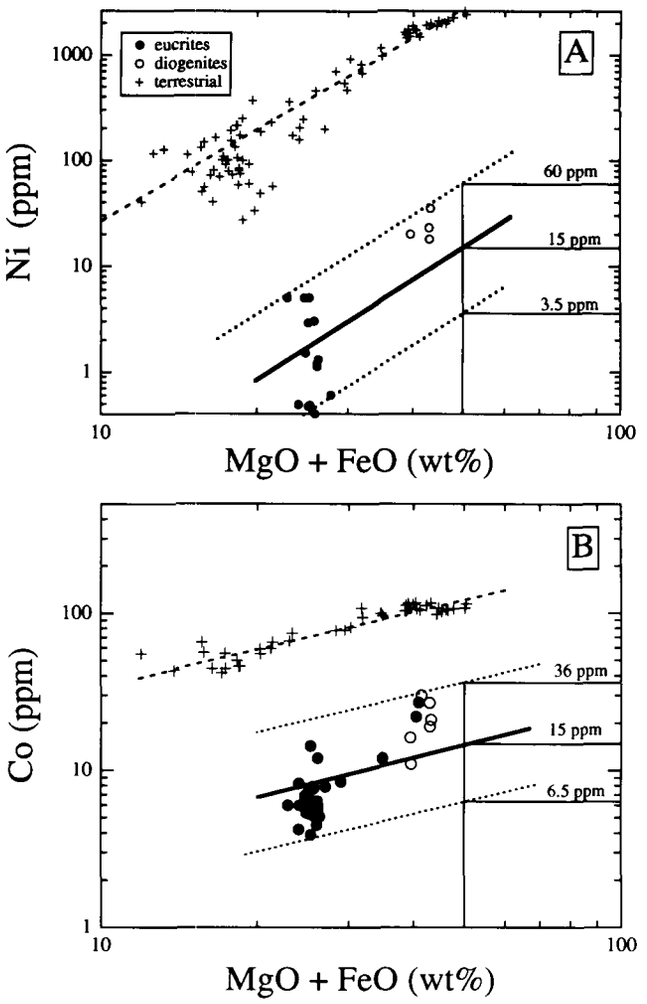

FIG. 1. Correlation diagrams for Ni (A) and Co (B) with (MgO + FeO), for both terrestrial basalts, komatiites, and peridotites (data from Jagoutz *et al.*, 1979; Crawford and Cameron, 1985; Arndt, 1986; Dickey *et al.*, 1977; Chen *et al.*, 1991; Whitford and Arndt, 1978; Kay *et al.*, 1970) and HED meteorites (*eucrites*: Wänke *et al.*, 1972, 1977; Palme *et al.*, 1978; Warren and Jerde, 1987; Mittlefehldt, 1979; *diogenites*: Wänke *et al.*, 1977; Mittlefehldt and Lindstrom, 1993). Vertical lines in each diagram illustrate the range of Ni and Co contents of a mantle with 50% MgO + FeO as an example. The range of estimated MgO + FeO contents of the HED parent body compositions is 45 to 55% MgO + FeO (Jones, 1984; Dreibus and Wänke, 1980; Morgan *et al.*, 1978).

elements during silicate melting. Nickel and Co concentrations in the HED parent body mantle are estimated using correlations with bulk MgO + FeO (Fig. 1); note the well-defined trend for terrestrial basalt and mantle peridotite. There is a greater range of Ni and Co concentrations in the HED suite; given the limited number of HED meteorite samples and the possibility of small amounts of metal contamination (polymict breccias will be susceptible to chondritic metal contamination), this is not surprising. The slope of the terrestrial samples in each case is approximated and applied to the HED suite to estimate the HED mantle Ni and Co contents.

Molybdenum, W and P concentrations (i) are estimated by correlations with a reference refractory lithophile incompatible element (r); here we will use both La and Ce (Fig. 2). Since terrestrial basalts and komatiites have the same W/Ce, Mo/Ce and P/La values as mantle peridotites, the eucrite basalts can be used to estimate these

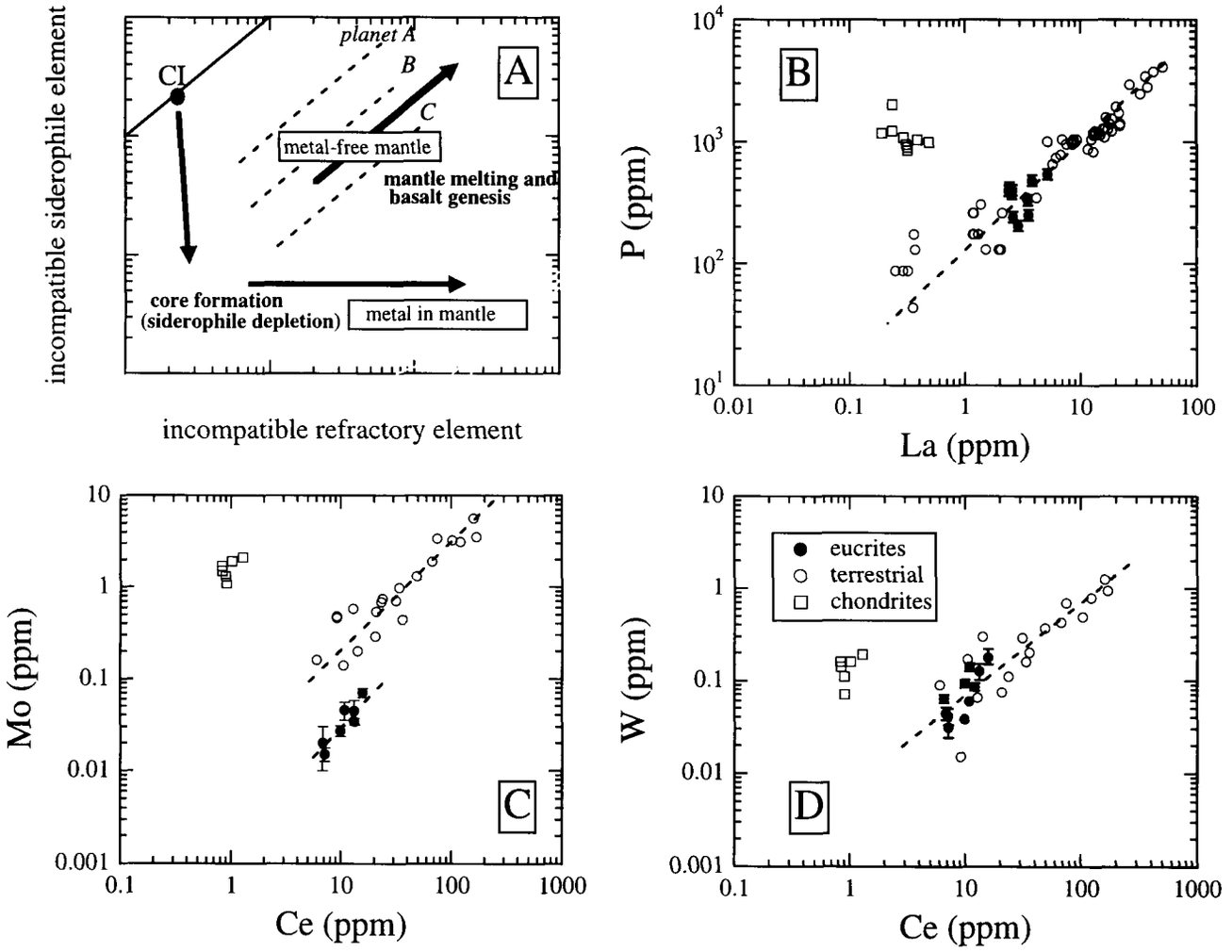

FIG. 2. (a) Hypothetical case illustrating the behavior of an incompatible siderophile element during core formation and later mantle melting. The behavior of incompatible siderophile elements during melting and fractionation processes in the absence of metal will produce straight lines of unity slope for a given planetary body. Molybdenum, W with Ce; in the presence of metal, a flat trend will result, due to the buffering effect of even a small amount of metal. (b) Phosphorus *vs.* La for both terrestrial basalts and peridotites (BVSP, 1981) and HED meteorites (Wänke *et al.*, 1972, 1977; Palme *et al.*, 1978; Mittlefehldt, 1987; Warren and Jerde, 1987; Fukuoka *et al.*, 1977; Mittlefehldt and Lindstrom, 1993; Warren *et al.*, 1990). (c) Molybdenum *vs.* Ce for both terrestrial basalts and peridotites (Sims *et al.*, 1990; Jochum *et al.*, 1989) and HED meteorites (Newsom, 1985; Morgan *et al.*, 1978; Palme and Ramensee, 1981; Schmitt *et al.*, 1964; Wänke *et al.*, 1977). (d) Tungsten *vs.* Ce for both terrestrial basalts and peridotites (Newsom *et al.*, 1996; Jochum *et al.*, 1989) and HED meteorites (Palme and Ramensee, 1981; Wänke *et al.*, 1972, 1974, 1977; Palme *et al.*, 1978; Morgan *et al.*, 1978).

ratios in the primitive eucrite parent body mantle. Knowing the basaltic ratios and the bulk mantle abundance of the reference refractory lithophile incompatible element (r, taken from Newsom, 1995 for a broad range of ordinary and carbonaceous chondrites), enables the calculation of the bulk mantle abundance of an incompatible siderophile element following core formation:

$$\frac{C_i^{mantle}}{C_r^{mantle}} = \frac{C_i^{basalt}}{C_r^{basalt}} \qquad \text{Eq. (1)}$$

There are seven data points for Mo and a cluster of twelve W data points for eucrites. A line of equal slope to the terrestrial data is forced through these points, which is allowable given the error bars associated with the data. Molybdenum and W chondritic data arguably have nearly the same slope as the basalt data; but since P/La ratios of chondrites are perpendicular to the basalt trends, the relative depletions of P are variable depending upon the specific chondritic composition considered. For this reason, there is a much greater range of P concentrations in the calculated mantles in Table 1. Primitive mantle abundances determined in this manner may be used in conjunction with metal-silicate partition coefficients and mass balance constraints to determine the conditions under which planetary cores formed.

Prediction of Metal-silicate Partition Coefficients

The partitioning of siderophile elements between metal and silicate liquid has been studied experimentally by many workers and is clearly a function of temperature, pressure, O_2 fugacity, nonmetal content of metallic liquid, and silicate liquid composition. If one considers an equilibrium expression of the following form:

$$\underset{\text{(metal)}}{M} + \frac{n}{4}\underset{\text{(gas)}}{O_2} = \underset{\text{(silicate liquid)}}{M^{n+}O_{n/2}} \qquad \text{Eq. (2)}$$

then at equilibrium:

$$\frac{-\Delta G^\circ}{RT} = \ln \frac{aM^{n+}O_{n/2}}{(aM)^*(fO_2)^{n/4}} \quad \text{Eq. (3)}$$

where ΔG° is the standard state free energy of the reaction, a is the thermodynamic activity of the chemical species, M is the metallic element of interest, and n is the valence of M in the silicate liquid (see *e.g.*, Capobianco *et al.*, 1993). The effect of temperature, pressure, O_2 fugacity and melt and metal composition has been quantified for specific siderophile elements by Righter *et al.* (1997) and Righter and Drake (1996), according to equations of the form:

$$\ln D = a \ln fO_2 + \frac{b}{T} + \frac{cP}{T} + d\frac{nbo}{t} + e\ln(1 - X_S) + f \quad \text{Eq. (4)}$$

The b, c and f terms result from the expansion of the above free energy term ($\Delta G^\circ = \Delta H^\circ - T\Delta S^\circ + P\Delta V^\circ$) and are related to $\Delta H^\circ/R$, $\Delta V^\circ/R$ and $\Delta S^\circ/R$, respectively. The a term is related to the valence of the element in the silicate melt. The d and e terms account for variations in silicate melt polymerization and metallic S content, respectively (see Righter *et al.*, 1997). Equations such as (4) can be used in the mass balance equations presented below.

Mass Balance Constraints

The distribution of a siderophile element (i) in a planetary body

TABLE 1. Summary of core formation models.

	H	L	LL	CI	CM	CO	CV
Bulk chondrite							
Ni (ppm)	16000	12000	10200	11000	12000	14000	13400
Co (ppm)	810	590	490	502	575	688	655
Mo (ppb)	1700	1300	1100	928	1177	1900	2100
W (ppb)	160	110	90‡	92.6	140	160	190
P (ppm)	1080	950	850	1220	900	1040	990
La (ppb)	295	310	315	235	317	387	486
Ce (ppb)	830	900	907	603	838	1020	1290
Estimated mantle							
Ni (ppm)	4–80	4–80	4–80	4–80	4–80	4–80	4–80
Co (ppm)	7–40	7–40	7–40	7–40	7–40	7–40	7–40
Mo (ppb)	2.5 (4.2,1.2)	2.7 (4.5,1.4)	2.7 (4.5,1.4)	1.8 (3.0,0.9)	2.5 (4.2,1.3)	3.1 (5.1,1.5)	3.9 (6.5,1.9)
W (ppb)	5.8 (12.5,2.5)	6.3 (13.5,2.7)	6.3 (13.6,2.7)	4.2 (9.0,1.8)	5.9 (12.6,2.5)	7.1 (15.3,3.1)	9.0 (19.4,3.9)
P (ppm)	35 (65, 18)	37 (68, 19)	38 (69, 19)	28 (52, 14)	38 (70 19)	46 (85, 23)	58 (107, 29)
Calculated mantle							
Ni (ppm)	119 (260, 55)	112 (241, 51)	98 (210, 45)	138 (290, 64)	125 (255, 58)	150 (315, 70)	207 (450, 70)
Co (ppm)	19 (40, 9)	15 (33, 7)	14 (30, 7)	15 (31, 7)	14 (30, 7)	21 (42, 10)	33 (70, 15)
Mo (ppb)	1.3 (3.1, 0.3)	1.5 (3.0, 0.4)	1.5 (2.7, 0.5)	1.4 (7.6, 0.3)	2.5 (13 0.5)	2.2 (12, 0.4)	2.0 (5.6, 0.4)
W (ppb)	12 (38, 2.6)	13 (34, 3)	12 (28, 3)	7.5 (14, 2.0)	12 (20, 4)	9.4 (20, 3)	17 (55, 4)
P (ppm)	62 (64, 55)	59 (61, 51)	55 (57, 50)	29 (30, 26)	20 (22, 18)	22 (24, 20)	104 (108, 92)
T (°C)	1527	1527	1527	1517	1507	1507	1530
Δ IW	–2.3	–2.2	–1.9	–2.4	–2.1	–2.4	–2.6
core mass (wt %)	15	18	20	15	25	12	5
fraction of mantle molten (p)*	0.77	0.77	0.74	0.68	0.65	0.65	0.72
fraction of core molten (m)*	0.99	0.99	0.99	0.96	0.94	0.94	0.99
X_S†	0.20	0.12	0.20	0.08	0.10	0.20	0.22

Columns represent the results of our modeling for specific chondrite compositions (tabulated by Newsom, 1995).
"Estimated mantle" values are calculated using chondrite siderophile element abundances and analyses of eucrites and diogenites (for Ni and Co, a range is given based on the trends in Fig. 1; the numbers in parentheses represent high and low mantle concentrations, based on the range of element ratios in Fig. 2). "Modeled mantle" values are calculated using the mass balance constraints of Eq. (1); numbers in parentheses represent high and low mantle concentrations, based on the 2σ error of the metal-silicate partition coefficient regressions.
*For both the metallic and silicate liquid systems, the fraction of molten material was estimated using the approach of McKenzie and Bickle (1988); if both liquidus and solidus temperatures (T_l and T_s, respectively) are known for the composition, then the fraction of molten material (p or m) can be estimated as a function of temperature by p (or m) = $T' + (T'^2 - 0.25)(a_0 + a_1 T') + 0.5$, where $a_0 = 0.4256$ and $a_1 = 2.988$, and

$$T = \frac{T - \frac{T_l - T_s}{2}}{T_l - T_s}$$

Values for T_l and T_s were taken from Agee *et al.* (1995), Takahashi (1983) and from Kubaschewski (1982).
†In cases where the temperature was below the liquidus surface of the Fe-S system, the liquid S content was constrained to be that required by the Fe-S phase diagram reported by Kubaschewski (1982). A polynomial fit to the liquidus surface is: $X_S = -2.1146 + (0.0041135)T - (1.6424 \times 10^{-6})T^2$, where T is in kelvins.
‡Tungsten concentration in LL chondrites was estimated based on trends in Ni, Co and Mo concentrations in the H-L chondrites.

that has undergone core formation can be understood in terms of the following mass balance equations:

$$C^i_{bulk} = xC^i_{sil} + (1-x)C^i_{met} \quad \text{Eq. (5)}$$

where

$$C^i_{sil} = pC^i_{LS} + (1-p)C^i_{SS} \quad \text{Eq. (6)}$$

and

$$C^i_{met} = mC^i_{LM} + (1-m)C^i_{SM} \quad \text{Eq. (7)}$$

Recasting Eqs. (6) and (7) in terms of C^i_{LS} produces:

$$C^i_{sil} = C^i_{LS}[p + (1-p)D^i{}_{SS/LS}] \quad \text{Eq. (8)}$$

and

$$C^i_{met} = C^i_{LS}[mD^i_{LM/LS} + (1-m)D^i_{SM/LS}] \quad \text{Eq. (9)}$$

Rearranging, and substitution of the latter expressions back into the first, gives:

$$C^i_{bulk} = x[C^i_{LS}[p + (1-p)D^i_{SS/LS}]] + (1-x)[C^i_{LS}[mD^i_{LM/LS} + (1-m)D^i_{SM/LS}]] \quad \text{Eq. (10)}$$

where x = silicate fraction of the planet; p = fraction of the silicate that is molten; and m = fraction of the metal that is molten; C^i_{met}, C^i_{sil}, and C^i_{bulk} are concentrations of siderophile elements in the metallic, silicate and bulk portions of the planet; $D^i_{LM/LS}$ is the liquid metal/liquid silicate partition coefficient, $D^i_{SM/LS}$ is the solid metal/liquid silicate partition coefficient, and $D^i_{SS/LS}$ is the solid silicate/liquid silicate partition coefficient.

Results of Modeling

The modeling approach is essentially the same as that presented by Righter and Drake (1996), with the exception that we will be investigating the sensitivity of our earlier conclusions to different bulk chondrite compositions (CI, CO, CM, CV, H, L, LL).

Equation (10) demonstrates that there are many variables involved in modeling core formation, even in a small body. Several of these variables are interdependent and, thus, can be linked in the modeling. For instance, the fractions of molten silicate and metal (p and m, respectively) will be related to temperature. In a study of the melting behavior of the terrestrial upper mantle, McKenzie and Bickle (1988) derived an expression for p based on temperature variations and knowledge of the liquidus and solidus temperatures (see Table 1). We have used this approach for estimating both p and m as a function of temperature in our calculations; chondrite liquidus and solidus temperatures were taken from Takahashi (1983) and Agee *et al.* (1995). Similarly, the S content of the metallic liquid (X_S) can be estimated as a function of temperature by fitting a polynomial to the liquidus surface of the Fe-S diagram (*e.g.*, Kubaschewski, 1982) (see Table 1). Using Eqs. (4) and (10), C^i_{sil} can be calculated for the five moderately siderophile elements at specific conditions to determine if the mantle abundances in Table 1 can be matched.

For a magma ocean scenario on a Vesta size body, central pressure (P) is not more than 2 kb, a magma ocean would be peridotitic (nbo/t = 2.8; the compositions for the estimated bulk HED parent body mantle are given in Table 2, and, if molten, all would be highly de-

TABLE 2. Comparison of estimated howardite, eucrite and diogenite parent body, chondrite and "post core mantle" compositions.

	1*	2*	3*	H	L	LL	CI	CO	CM	CV	0.25CV − 0.75H	0.30CV − 0.70L	0.30CM − 0.70H	0.36CM − 0.64L
Bulk chondrite†														
SiO_2				36.4	41.3	43.4	34.0	35.6	35.1	35.4	36.0	38.3	34.4	35.5
TiO_2				0.10	0.11	0.11	0.11	0.14	0.12	0.17	0.13	0.15	0.12	0.14
Al_2O_3				2.15	2.38	2.40	2.51	2.83	2.84	3.51	2.42	2.84	2.14	2.42
Cr_2O_3				0.54	0.59	0.58	0.59	0.54	0.57	0.56	0.51	0.50	0.50	0.49
FeO				35.65	28.57	25.41	36.16	33.41	34.39	32.06	33.92	26.89	33.05	26.45
MnO				0.30	0.34	0.36	0.39	0.22	0.28	0.20	0.28	0.30	0.28	0.29
MgO				23.38	25.17	26.20	24.58	25.17	24.69	25.49	23.59	25.13	22.25	23.05
CaO				1.76	1.89	1.91	2.03	2.31	2.26	2.82	1.95	2.16	1.78	1.92
Na_2O				0.87	0.97	1.01	1.04	0.59	0.70	0.47	0.75	0.75	0.67	0.62
K_2O				0.09	0.10	0.10	0.10	0.04	0.06	0.04	0.08	0.08	0.08	0.08
% core mass				15	18	20	15	12	25	5	12	14	18	21
Mantle (post-core)‡														
SiO_2	40.3	39.8	46.2	41.2	49.7	54.2	41.4	38.7	48.7	37.4	40.3	46.1	43.5	49.4
TiO_2	0.16	0.13	0.16	0.11	0.13	0.14	0.13	0.15	0.17	0.18	0.13	0.15	0.13	0.15
Al_2O_3	3.2	2.5	3.27	2.44	2.87	3.00	3.06	3.08	3.93	3.71	2.75	3.12	2.89	3.25
Cr_2O_3	0.34	—	0.87	0.61	0.71	0.73	0.71	0.59	0.79	0.59	0.61	0.67	0.66	0.73
FeO	25.2	26.6	14.8	27.15	13.96	4.98	22.26	27.55	9.08	28.14	27.40	18.21	21.73	12.20
MnO	0.63	0.018	0.42	0.40	0.44	0.45	0.33	0.28	0.29	0.25	0.36	0.38	0.37	0.39
MgO	27.7	28.5	31.5	26.47	30.31	32.73	29.93	27.38	34.22	26.97	26.60	29.31	28.80	31.72
CaO	2.6	2.06	2.57	2.00	2.28	2.39	2.47	2.52	3.14	2.98	2.24	2.49	2.34	2.59
Na_2O	0.11	0.05	0.11	1.15	1.26	1.26	0.90	0.74	0.74	0.59	1.01	1.06	1.03	1.07
K_2O	0.010	0.004	0.0092	0.13	0.13	0.13	0.09	0.06	0.06	0.05	0.11	0.11	0.11	0.11
Mg# (molar)				0.63	0.79	0.92	0.71	0.64	0.87	0.63	0.63	0.74	0.70	0.82

*HED bulk compositions reported by (1) Jones (1984); (2) Morgan *et al.* (1978); (3) Dreibus and Wanke (1980).
†Chondrite bulk major and trace element data is from the compilation of Newsom (1995); all Fe is reported as FeO.
‡"Post core mantle" compositions were calculated from results of core modelling presented in Table 1.

polymerized silicate melts). The O_2 fugacity is known to be lower than the iron-wüstite buffer (IW); these variables can be fixed in the calculations. Coefficients for calculating metal-silicate partition coefficients, $D^i_{LM/LS}$ and $D^i_{SM/LS}$ are from Righter *et al.* (1997), and the solid silicate/liquid silicate partition coefficients, $D^i_{SS/LS}$ are taken from the compilation of Green (1994). The remaining variables are bulk composition (C^i_{bulk}), core size (1–x), and temperature (T), with the latter linked to p, m and X_S as described above.

The results are tabulated in Table 1 and indicate that even with a range of ordinary and carbonaceous chondrite starting materials, estimated siderophile element abundances in the HED mantle are consistent with separation of a small core at high (silicate liquidus) temperatures. The estimated and calculated values presented in Table 1 agree within a factor of two, which is well within the error associated with the partition coefficient regressions (Eq. (4)). The temperatures range from 1500 to 1530 °C, mostly molten mantle (p = 0.65 to 0.77) and mostly molten metal (m = 0.94 to 1.00). The core sizes range from 5 to 25% by mass, and the Ni contents range from 4.8 to 22 wt%, which overlap with the range of Ni contents reported for iron meteorite groups (*e.g.*, Buchwald, 1977). Sulfur mass balance in a small asteroid with a metallic core can be calculated using the S concentrations reported by Dreibus *et al.* (1995). For example, many chondrites contain ~2 wt% S; segregation of a 15% by mass metallic core would result in a core with ~12 wt% S, or approximately X_S = 0.20, which is in good agreement with our results (Table 1).

We may draw two conclusions from this modeling exercise. First, the abundances of the moderately siderophile elements in the HED parent body mantle may be produced in a magma ocean environment from a variety of plausible primitive compositions. Second, the results require a small core (5 to 25% by mass) to have separated, which is in contrast to the rather sizable core calculated by Newsom (1985), 40–50% by mass.

CRYSTALLIZATION OF A MAGMA OCEAN

Physical Aspects: Convection and Crystal Suspension

The concept of a planetary magma ocean has been incorporated into models for the origin of the Moon and Earth (*e.g.*, Warren, 1985b). The specific physical setting will have a great impact on the nature of magmatic crystallization processes, whether fractional or equilibrium crystallization. The convective vigor of a magmatic system can be characterized in terms of the dimensionless Rayleigh number,

$$Ra = \frac{\alpha\rho\, gHD^5}{Kkv} \qquad \text{Eq. (11)}$$

and the importance of thermal diffusion in regulating the flow is measured by the Prandtl number,

$$Pr = \frac{v}{k} \qquad \text{Eq. (12)}$$

where α is the thermal expansion coefficient, ρ is the fluid density, g is the acceleration due to gravity, H is the rate of internal heat generation per unit mass, D is the depth of convecting fluid, K is the thermal conductivity of the fluid, k is the thermal diffusivity of the fluid, and v is the kinematic viscosity (viscosity/density). High Rayleigh numbers ($>10^{20}$) are characteristic of a system that will convect vigorously, while high Prandtl numbers occur in systems with a relatively high convective momentum relative to conductive heat loss. In systems that convect vigorously, there exist several dynamic regions, including conductive boundary layers, viscous sublayers, and inertial flow zones (Fig. 3a). Crystals will be entrained in the inertial flow zone in conditions of high Ra and low Pr (turbulent flow; high velocity), while they will tend to settle out in conditions of low Ra and high Pr (laminar flow; low velocity). A boundary between these two regimes (laminar and turbulent) has been defined by Kraichnan (1962) according to the relation, $Ra^{1/2} = 35Pr^{1/3}$. Many magma chambers undergo fractional crystallization as opposed to equilibrium, since they straddle the laminar flow regime (Fig. 3b; see also Spera, 1992). Also note the position of the subsolidus convecting terrestrial mantle deep in the laminar flow region. Magma oceans will be largely in the turbulent regime, unless the degree of crystallinity becomes large enough to reduce the Ra number into the laminar regime.

Another important variable in controlling particle suspension in fluids is grain size. This issue is common to magmas, fluvial sediment, and airborne dust (Tonks and Melosh, 1990); there exists a critical grain size above which there will be particle settling. It was this kind of assessment that led Tonks and Melosh (1990) and Taylor *et al.* (1993) to the conclusion that terrestrial magma oceans can suspend crystals at up to 50% crystallization (before convective lockup). Several aspects of an asteroid magma ocean will foster an even greater fraction of crystal suspension during cooling. First, the acceleration due to gravity on a small asteroid will be nearly two orders of magnitude smaller (~0.1 m/s^2) than that on Earth. Gravitational segregation will, thus, take place at a higher degree of crystallization. Second, the slope of the adiabat will closely parallel the liquidus and solidus, as opposed to terrestrial or lunar adiabats that are steeper than the liquidus and solidus slopes (*e.g.*, Tonks and Melosh, 1990). The Earth/Moon cases favor subliquidus conditions at the base of a magma ocean and superliquidus conditions near the top; cooling along an asteroid adiabat, however, would produce subliquidus temperatures at all depths. This condition would produce crystals of equal size during cooling, rather than a range of sizes. Finally, it is important to recognize that crystallization in magma chambers (usually dominantly fractional crystallization) is controlled by the thermal effects of both roof and wall rock (*e.g.*, Marsh, 1988; Spera, 1992; Martin and Nokes, 1988); the greater scale and lack of thermal wall effects in a magma ocean should help to suppress fractional crystallization.

Compositional Aspects

Mantle Composition After Core Formation–Having demonstrated above that the HED parent body may have a small core (5 to 25% by mass) that separated during a global magma ocean episode (65 to 77% melting; 1500–1530 °C), we can now evaluate whether the eucrites and diogenites may represent the residual liquids and cumulates formed during the crystallization of such an ocean. The HED parent body mantle composition will be different than the bulk chondritic composition after separation of an Fe-rich metallic core, even if the core is small (5 to 10% by mass; see Table 2). The most important difference will be the Mg/(Mg + Fe) ratio (Mg#) of the mantle material; separation of a metallic core will increase this ratio over the bulk chondritic value, thus having a significant impact on the composition of phases crystallizing from a magma ocean (see "chondrite minus core" in Table 2). To illustrate this difference, we have tabulated several chondritic bulk compositions and the resulting mantle compositions after separation of a metallic core of the size and composition predicted in our calculations from the previous section (Tables 1 and 2).

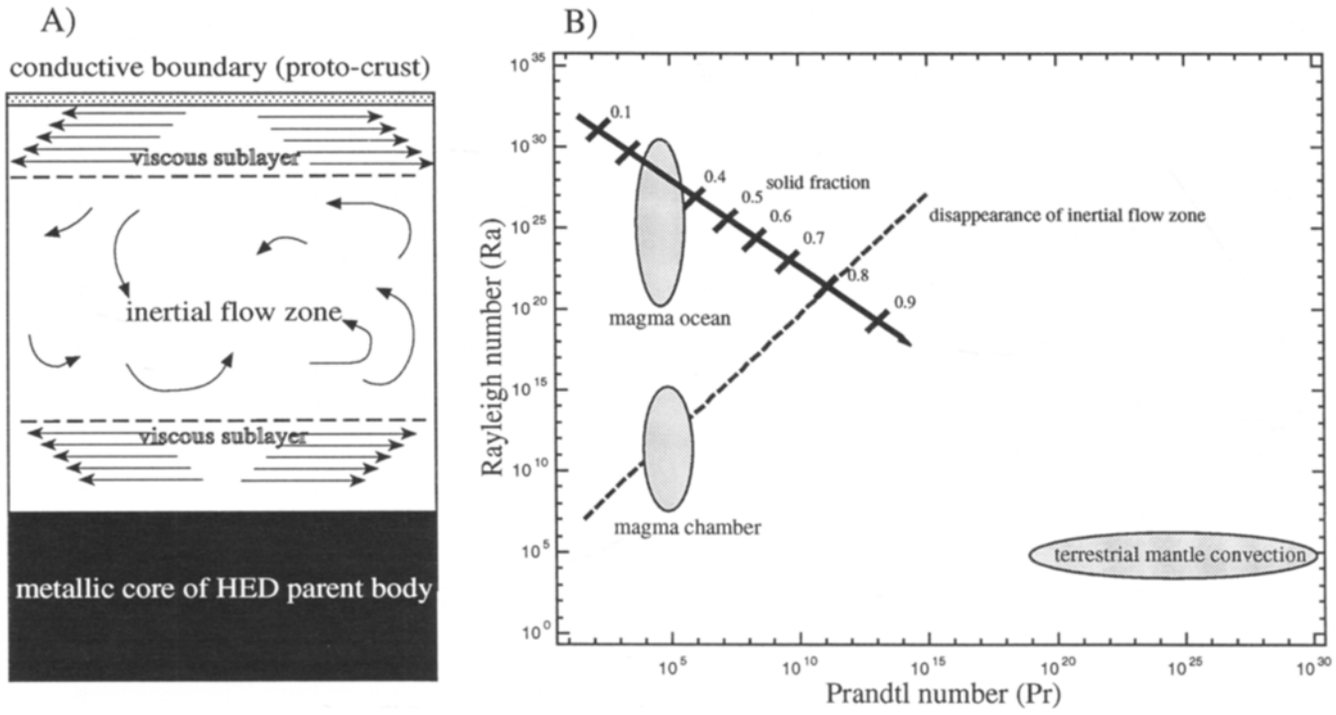

FIG. 3. (a) Structure of a convecting system including conductive boundary layer, viscous sublayer, and inertial flow zone (after Spera, 1992), with the bottom of the magma ocean floored by a metallic core in the specific case considered in this study. (b) Rayleigh number *vs.* Prandtl number for magma chambers, magma oceans and terrestrial subsolidus mantle convection (after Tonks and Melosh, 1990). The change over from turbulent to laminar flow and the disappearance of the inertial flow zone is denoted by a dashed line and taken from Kraichnan (1962). The calculated trajectory of the magma ocean is shown by a solid heavy line with tick marks indicated at 0.1 fractions. The Ra and Pr numbers for the trajectory were calculated using the viscosities and densities in Table 3 and the following additional values: $\alpha = 3 \times 10^{-5}$ K^{-1}, g = 10 cm/s^2, H = 1 erg, D = 100 km, K is temperature dependent from 3.0 to 0.4 $\times$ 10^4 erg/s (Snyder *et al.*, 1994), and k = 0.01 cm^2/s.

A second mantle compositional difference after core formation will be the Fe/Mn ratio. Since Fe partitions readily into a metallic core and Mn does not (D(Mn) metal/silicate <0.1; Drake *et al.*, 1989), the Fe/Mn ratio in the residual mantle will decrease significantly from the original chondritic values. Ratios of Fe/Mn in eucrites are narrowly defined from 30 to 45 (Boesenberg and Delaney, 1997) and, thus, must be satisfied in any successful model of eucrite petrogenesis. Finally, any bulk composition chosen for the HED parent body must have the same O isotope values as eucrites and diogenites. These constraints have formed the basis of previous studies, and the O isotope composition of the HED parent body can be produced by mixing carbonaceous (CV, CM) and ordinary (H, L, LL) chondrite materials (Boesenberg and Delaney, 1997). We will show below that all three of these compositional constraints can be met if a 0.3CV-0.7L mixture is considered as the bulk starting material of the HED parent body.

A final characteristic of postcore chondritic materials is the high volatile element contents, and especially Na_2O and K_2O. Concentrations of these oxides in the calculated mantle compositions range from 0.8 to 1.2% (Na_2O) and 0.09 to 0.11% (K_2O). Previous estimates of HED parent body compositions have noted the volatile element depletions relative to all chondrites, as much as 0.1 $\times$ CI; the bulk composition reported by Dreibus and Wänke (1980), for instance, contains 0.11% Na_2O. The significance of these depletions will be discussed in some detail below; for the modelling presented below, Na_2O and K_2O contents of 0.11 and 0.01% are used in the mantle compositions.

Fractional or Equilibrium Crystallization?–The compositional evolution of a silicate melt undergoing either equilibrium or fractional crystallization can be predicted using two different techniques: phase equilibrium or thermodynamics. The work of Longhi (1987) and Longhi and Pan (1988) offers an opportunity to use the former approach (using the computer programs MAGFOX or MAGPOX for fractional or equilibrium crystallization, respectively), and a recent calibration of a regular solution model for silicate melts (Ghiorso and Sack, 1995) offers an opportunity for the latter (using the computer program MELTS). MELTS is calibrated on nearly 2500 solid-liquid experiments, including many of the experimental data collected on eucrites and chondrites (*e.g.*, Stolper, 1977; Bartels and Grove, 1991; Grove and Bartels, 1992; Longhi and Pan, 1988; Jurewicz *et al.*, 1991, 1995).

Recent work by Ruzicka *et al.* (1996, 1997) has suggested that the eucrites formed by fractional crystallization of a magma ocean with the composition reported by Dreibus and Wänke (1980). Their modelling is based on the MAGFOX (Longhi, 1987) computer program. Although the physical conditions prevailing in a magma ocean stage seem to favor equilibrium crystallization processes rather than fractional crystallization (see above discussion), we have calculated liquid lines of descent for fractionation of the HED bulk composition reported by Dreibus and Wänke (1980), which was used by Ruzicka *et al.* (1996, 1997), to demonstrate the compositional differences of the residual liquids calculated using both the MAGFOX and MELTS models. We show (Fig. 4) that the liquid trends are not eucritic regardless of whether the calculations are done with MELTS

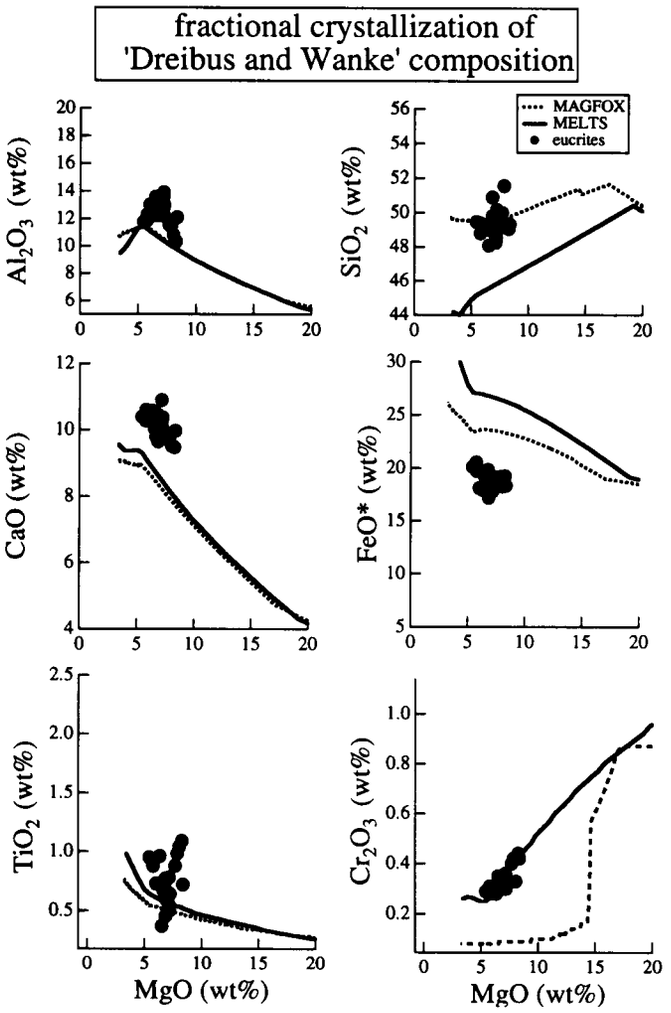

FIG. 4. Calculated liquid lines of descent for *fractional* crystallization of Dreibus and Wänke (1980) bulk HED composition using both MELTS (solid line) and MAGFOX (dashed line) compared to eucrites and eucritic clasts (solid symbols). All trends begin at 1500 °C and end at 1125 °C (calculations done at 1 bar pressure). Note the mismatch between both calculated trends and eucritic FeO* and CaO (eucrite composition data taken from BVSP, 1981; Wänke *et al.*, 1972, 1974, 1977; Palme *et al.*, 1978; Mittlefehldt, 1987; Warren and Jerde, 1987; Fukuoka *et al.*, 1977; Mittlefehldt and Lindstrom, 1993; Warren *et al.*, 1990; Morgan *et al.*, 1978; Palme and Ramensee, 1981; Schmitt *et al.*, 1964; Warren *et al.*, 1996).

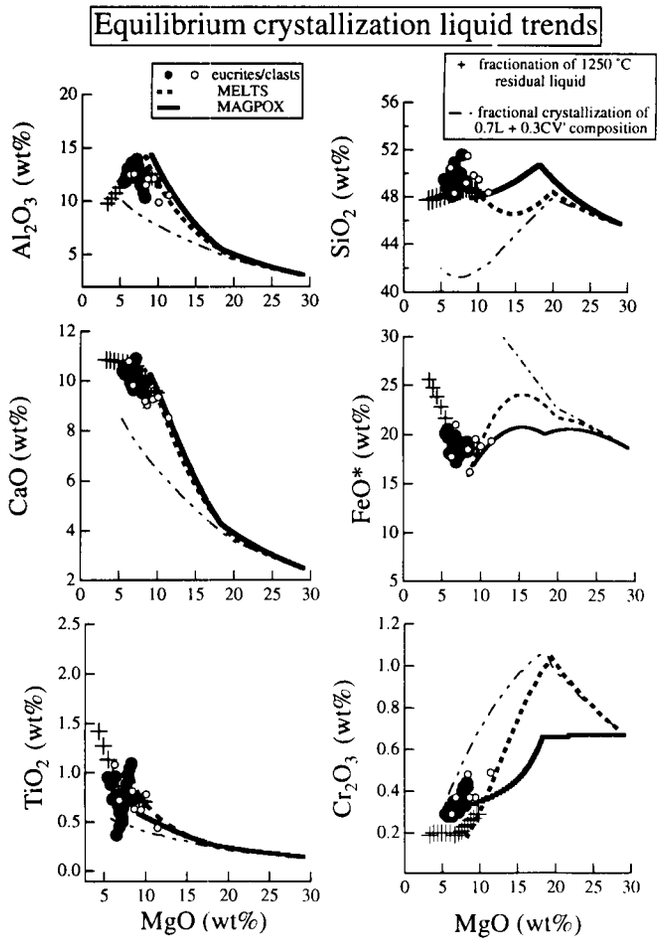

FIG. 5. Major element variation diagrams showing *equilibrium* crystallization trends of 0.7L + 0.3 CV chondrite liquid calculated using MELTS (solid line) and MAGPOX (dashed line), and eucritic clasts (open circles; Mittlefehldt, 1979; Buchanan and Reid, 1996, Mittlefehldt and Lindstrom, 1997) and eucritic basalts (solid circles; same samples from Fig. 4). Calculations were done at a fixed pressure of 500 bar, from 1530 to 1150 °C, with O fugacity buffered at the iron-wüstite (IW) buffer. Also shown is the calculated liquid trend (using MELTS) for fractional crystallization (crosses) of a residual liquid produced during equilibrium crystallization; the initial liquid in this trend is from 1250 °C. The dot-dash pattern is the liquid trend produced by fractional crystallization of the L-CV chondrite mixture; as with the composition modeled in Fig. 4, it does not produce eucritic liquids either. The equilibrium crystallization trends begin at 1530 °C and stop at 1180 °C.

or MAGFOX; the *fractional* crystallization trends become too FeO-rich at the eucritic SiO_2 and MgO contents. In fact, none of the ordinary-carbonaceous chondrite compositions that satisfies O isotope constraints can produce eucritic liquids during a fractionation series; the residual liquids produced during fractionation of an LL-CM mix are too SiO_2-rich and low in MgO and FeO; those produced during fractionation of L-CV and L-CM mixes are too FeO-rich and low in MgO, SiO_2 and Al_2O_3. Liquids produced by *equilibrium* crystallization of chondritic compositions come close to eucritic liquids at 80–85% crystallization (Fig. 5). The composition considered below is a mixture of ordinary and carbonaceous chondrites (0.7L + 0.3 CV) and satisfies Fe/Mn and O isotope constraints for the HED parent body.

A COMPREHENSIVE MODEL

Step 1: Initial Crystallization of the Magma Ocean

Both equilibrium and fractionation crystallization calculations were done with a mixture of 0.7L + 0.3 CV chondrite starting melt compositions (adjusted for core separation), at 500 bar, and from 1530 to 1150 °C, with O_2 fugacity buffered at the iron-wüstite (IW) buffer. The MELTS program is not designed to calculate O_2 fugacities lower than the IW buffer, but the calculations in the previous section indicate that core formation in the HED parent body may have commenced at O_2 fugacities as low as $2\log fO_2$ units below the IW buffer. Although there will be more FeO stable at the lower fO_2 conditions, the difference between IW and IW-2 is minor; according to the expression of Kress and Carmichael (1991), the Stannern eucrite (17.9% FeO*) will have 17.4% FeO stable at the IW buffer and 17.7% FeO stable at IW-2. Since a core has already separated from this material, there is no metal left during mantle crystallization.

As with the Dreibus and Wänke (1980) mantle composition from the previous section, *fractional* crystallization of the L-CV chondritic melt composition produces liquids that are much more FeO- and TiO_2-rich, and MgO-poor than eucrites and, thus, cannot be the pro-

cess by which the eucrites formed (Fig. 5). However, 80% *equilibrium* crystallization of a mantle originating from a mixture of ordinary-carbonaceous chondrite material (0.7L + 0.3 CV, adjusted for core separation) produces a melt composition virtually indistinguishable from a Main Group eucrite in terms of SiO_2, TiO_2, Al_2O_3, Cr_2O_3, FeO, MgO and CaO (Table 3; Fig. 5). Olivine, spinel and orthopyroxene are stable crystallizing phases from 1530 to ~1240 °C, at which point pigeonite becomes stable and replaces orthopyroxene as the crystallizing pyroxene until ~1150 °C (Fig. 6). From 1230 to 1180 °C, orthopyroxene and spinel crystallize with minor amounts of olivine, the phases represented in diogenites (Hewins, 1981). A fundamental point of contention in past models for diogenite genesis has been whether the Mg# of the proposed fractionated minerals (cumulates) can be reconciled with the Mg# of the cumulate diogenites and diogenitic clasts in howardites (*e.g.*, Bartels and Grove, 1991; Grove and Bartels, 1992; Jurewicz *et al.*, 1995; Fowler *et al.*, 1995). The Mg#s of the pyroxene crystallizing to form the eucrite liquids are plotted for comparison to the range of Mg# in pyroxene from diogenites and howardites in Fig. 7; there is nearly complete overlap. Although diogenite pyroxene Mg#s may have been reset from their original igneous values, minor refractory element (Al, Ti) concentrations also show ranges that are consistent with an igneous fractionation trend (*e.g.*, Fowler *et al.*, 1994; Mittlefehldt, 1994).

Further constraints are provided by consideration of trace element modeling. The Main Group eucrites and chondrites have been analyzed for a wide range of compatible (Sc, V and Cr) and incompatible (Ba, Sr, Zr, Y, REE and Lu) trace elements, and these data can be used to test the major element modeling above. If equilibrium crystallization of olivine, pyroxene and spinel in an L-CV chondritic magma ocean can account for the major element characteristics of the Main Group and Stannern trend eucrites, then the concentrations of trace elements in the residual liquid (C_{liq}) should be consistent with the following mass balance:

$$C_{liq} = \frac{C_o}{x_{liq} + D(1 - x_{liq})} \qquad \text{Eq. (13)}$$

where C_o is the initial chondritic abundance of the element, x_{liq} is the mass fraction of liquid, and D is the bulk solid/liquid partition coefficient defined as: $D = \Sigma X_i D_i$, for each phase, i. Using the average chondrite elemental abundances tabulated by Newsom (1995), the calculated mass fractions of liquid, olivine, pyroxene and spinel from the previous section, and partition coefficient data from Green (1994) and Horn *et al.* (1994), the concentration of these elements in the residual liquid can be calculated according to Eq. (13). Since the molar Mg/(Mg + Fe) ratio of a melt is sensitive to the degree of evolution of a magmatic system, incompatible elements are commonly plotted against this parameter to illustrate crystallization trends (*e.g.*, Warren and Jerde, 1987). Comparison of calculated trends with trace element analyses of eucrites shows that the elements Sc, Zr, Sm, Lu, Hf and Fe/Mn are all consistent with an origin of Main Group and Stannern trend eucrites by equilibrium crystallization of an L-CV chondrite mixture (Fig. 8).

In addition, trends of diogenite Mg# with trace element concentrations such as Yb and Sc indicate that the compositions of most of the diogenites are consistent with an igneous process (Mittlefehldt, 1994). Modelling of two incompatible refractory elements, Ti and Yb, also is consistent with equilibrium crystallization of a chondritic magma ocean. The trend expected for equilibrium crystallization is nearly identical to the trend defined by eucrites and calculated parent liquids to the diogenites (Fowler *et al.*, 1995; Fig. 9). The range recorded in the diogenite pyroxene cores reflects early to late pyroxene

TABLE 3. Liquids produced during equilibrium crystallization (0.5 kb, IW buffer) of 0.7L + 0.3CV mantle composition (adjusted for core separation).

Liquid fraction	T °C	SiO_2	TiO_2	Al_2O_3	Cr_2O_3	FeO	MgO	CaO	Na_2O	olivine Mg#	pyroxene Mg#	liquid viscosity (log Poise)	liquid density (g/cc)	solid density (g/cc)
1.00	1600	46.1	0.15	3.12	0.67	18.21	29.31	2.49	0.11	—	—			
0.70	1500	47.9	0.21	4.41	0.95	21.51	21.26	3.49	0.16	0.88	—	0.25	2.87	3.18
0.46	1400	46.8	0.32	6.30	0.86	23.92	16.40	5.08	0.24	0.83	0.84	0.61	2.91	3.23
0.44	1390	46.7	0.33	6.56	0.82	24.03	15.92	5.31	0.25	0.82	0.83	0.65	2.91	3.23
0.42	1380	46.6	0.35	6.84	0.78	24.07	15.44	5.55	0.26	0.81	0.82	0.70	2.91	3.24
0.40	1370	46.6	0.37	7.13	0.74	24.04	14.97	5.80	0.28	0.81	0.82	0.76	2.91	3.25
0.37	1360	46.6	0.39	7.43	0.70	23.95	14.50	6.06	0.29	0.80	0.81	0.81	2.91	3.25
0.35	1350	46.6	0.41	7.75	0.66	23.79	14.05	6.33	0.31	0.80	0.81	0.88	2.91	3.26
0.33	1340	46.7	0.43	8.08	0.62	23.56	13.60	6.61	0.33	0.79	0.80	0.94	2.91	3.27
0.32	1330	46.8	0.45	8.44	0.58	23.25	13.15	6.90	0.34	0.78	0.80	1.02	2.90	3.27
0.30	1320	46.9	0.48	8.81	0.54	22.87	12.71	7.21	0.37	0.78	0.79	1.09	2.89	3.28
0.28	1310	47.1	0.50	9.20	0.50	22.44	12.28	7.52	0.39	0.77	0.78	1.17	2.89	3.29
0.26	1300	47.3	0.53	9.61	0.46	21.93	11.85	7.85	0.41	0.77	0.78	1.26	2.88	3.29
0.25	1290	47.5	0.56	10.04	0.42	21.37	11.43	8.18	0.44	0.76	0.77	1.35	2.87	3.30
0.23	1280	47.7	0.59	10.48	0.39	20.76	11.02	8.51	0.47	0.75	0.76	1.44	2.86	3.30
0.22	1270	47.9	0.63	10.94	0.35	20.10	10.62	8.85	0.50	0.75	0.75	1.54	2.85	3.31
0.20	1260	48.1	0.66	11.41	0.32	19.42	10.23	9.19	0.53	0.75	0.75	1.64	2.84	3.31
0.19	1250	48.4	0.70	11.90	0.29	18.71	9.85	9.52	0.57	0.75	0.75	1.74	2.83	3.32
0.18	1240	48.6	0.75	12.39	0.26	17.98	9.48	9.85	0.61	0.74	0.75	1.85	2.82	3.32
0.16	1230	48.8	0.79	12.89	0.24	17.25	9.12	10.16	0.65	0.74	0.74	1.95	2.81	3.32
0.15	1220	49.0	0.85	13.39	0.21	16.54	8.76	10.47	0.71	0.74	0.73	2.06	2.80	3.33
0.11	1210	49.5	1.01	14.37	0.18	15.25	8.26	10.43	0.90	0.74	*0.73/0.67*	2.23	2.78	3.33
0.08	1200	50.1	1.19	15.34	0.15	13.97	7.70	10.20	1.20	0.74	*0.73/0.67*	2.42	2.75	3.33
0.05	1190	50.7	1.52	15.85	0.13	13.00	7.14	9.90	1.55	0.74	*0.66*	2.59	2.73	3.32
0.03	1180	51.3	2.17	16.00	0.12	11.94	6.55	9.62	1.66	0.73	*0.66*	2.77	2.71	3.32

Italicized pyroxene Mg#s are for pigeonite; all others are for orthopyroxene.

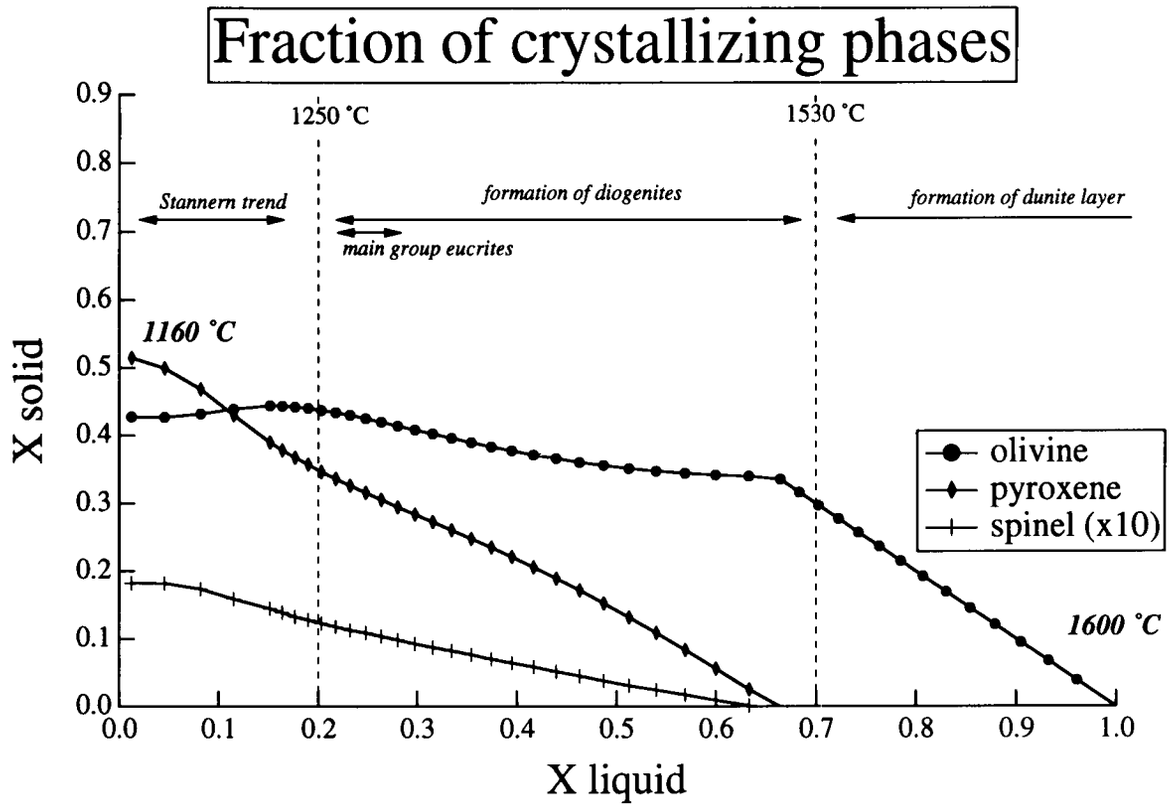

FIG. 6. Mass fraction of solids precipitated during equilibrium crystallization of 0.7L + 0.3 CV chondrite liquid calculated using MELTS. Note that olivine is the liquidus phase; from 1300 to 1200 °C, olivine is resorbed while pyroxene is the dominant crystallizing phase, which is exactly the conditions needed for the formation of diogenites.

growth. The refractory nature of Yb and Ti prevents reequilibration and thus these "magma ocean values" are locked into the pyroxene cores. This is evidence that the diogenites came from not a single parent liquid but rather an evolving, crystallizing magmatic system. The composition of the calculated liquid in equilibrium with the diogenitic cumulates is relatively MgO-rich (10–14%) and Al_2O_3-poor (7 to 11%), which is consistent with previous suggestions that the diogenite parent liquid may have had a more basic composition than a eucrite (Schwandt and McKay, 1996; Fowler *et al.*, 1995; Shearer *et al.*, 1996).

Step 2: Convective Lockup and Extrusion of Liquids

We now consider the physical aspects of the magma ocean. As discussed above, Tonks and Melosh (1990) and later Abe (1992) and Taylor *et al.* (1993) showed that, during a magma ocean stage, crystals can be suspended in a convecting solid-liquid mush until a critical melt fraction is attained, whereby the viscosity becomes large enough for gravitational separation of solid from liquid silicate to occur. Using the results of the MELTS compositional modelling, the Ra and Pr numbers (Eqs. 11 and 12) can be calculated from the liquid viscosities (calculated after Bottinga and Weill, 1972), magma viscosities according to the relation η (magma) = η (liquid) * $e^{23.03\phi}$ (where ϕ is the crystal fraction; Murase and McBirney, 1973), solid and liquid densities (calculated after Lange and Carmichael, 1987), $\alpha = 3 \times 10^{-5}$ K^{-1}, g = 10 cm/s^2, H = 1 erg, D = 100 km, K is temperature dependent from 3.0 to 0.4 $\times$ 10^4 erg/s (Snyder *et al.*, 1994), and k = 0.01 cm^2/s. Rayleigh and Prandtl numbers are calculated for the entire crystallization sequence from nearly 100% melt to complete solidification (Fig. 3b); the point at which the system makes the transition from turbulent to laminar flow corresponds to a crystal fraction of ~0.80 (Fig. 3b). The residual liquid at this degree of crystallinity is nearly identical in composition to that of a Main Group eucrite (see previous section).

Once this melt fraction is attained, crystal entrainment will stop (convective lockup), and melt will begin segregating from crystals and rise buoyantly to the surface. The ultimate effect will be to extrude a residual liquid toward the surface, thus forming a crudely layered mantle dominated by dunite at depth (the initial magma ocean had a small percentage of olivine that could have grown large enough to settle out first) and grading upwards into harzburgite (diogenite) and eucritic melt at the surface.

Step 3: Fractionation of Main Group Eucrites to Produce Cumulates and Nuevo Laredo Trend Liquids

Thermal modelling of Vesta size asteroids (Ghosh and McSween, 1996) as well as generalized magma ocean models (Spera, 1992) predict the existence of a thin, upper conductive boundary layer or solid crust. If such a crust formed early, its composition may be primitive and nearly chondritic (but metal-free). No meteorites have been recovered with such characteristics; however, there are ultramafic clasts (~24% MgO, 3.5% Al_2O_3 and 2.8% CaO) in the Kapoeta howardite (Smith and Schmitt, 1982) that are ~2× chondritic in terms of REE and trace elements and resemble some of the early liquids produced during equilibrium crystallization (Fig. 5). These howardite clasts may be remnants of such a thin early protocrust.

Any residual liquid from a magma ocean will be squeezed toward the surface and extruded or perhaps intruded into this thin solid crustal layer (*e.g.*, Wilson and Keil, 1996). This is a plausible

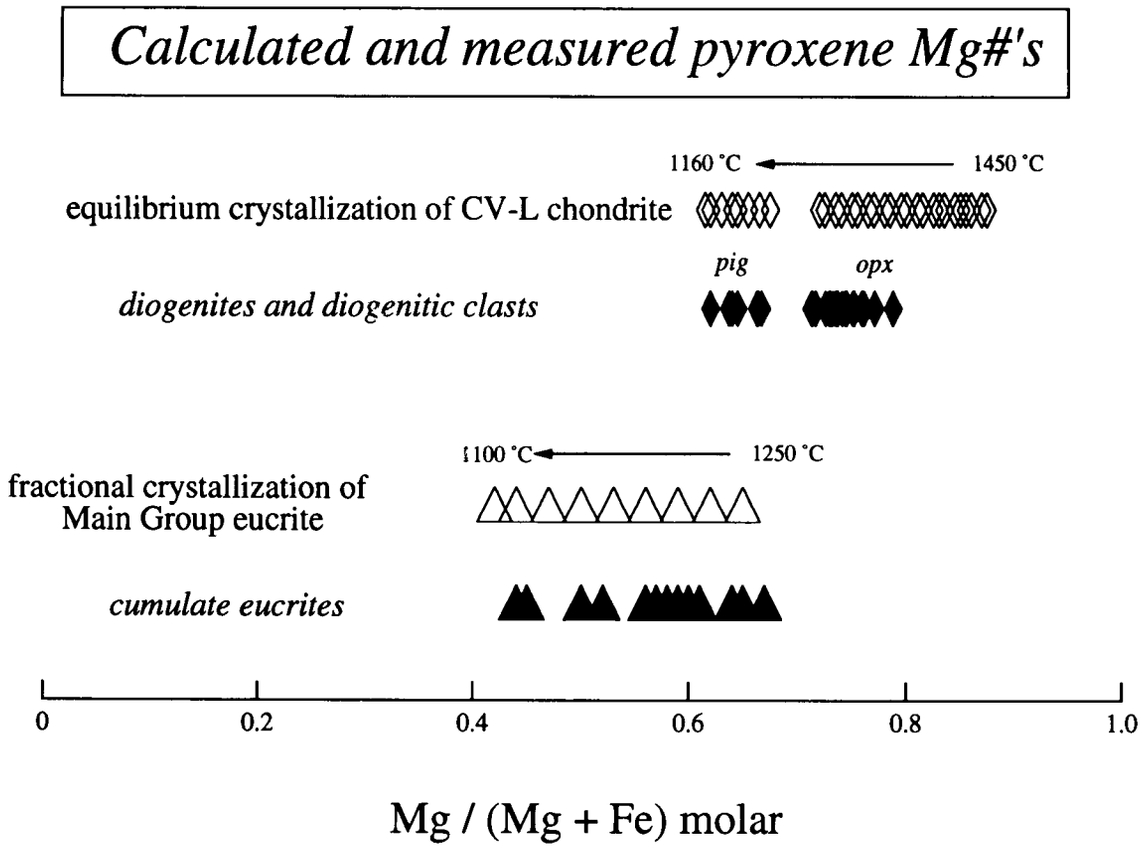

FIG. 7. Comparison of diogenite orthopyroxene and pigeonite Mg# (solid diamonds) with calculated pyroxene Mg# from an equilibrium crystallization trend (from 1450 to 1180 °C; open diamonds; Table 3). Diogenite data are from Fowler *et al.* (1994) and Sack *et al.* (1991), and diogenitic clasts are from howardites studies by Takeda (1986) and Takeda and Mori (1985). Also shown are cumulate eucrite pyroxene Mg#s (solid triangles) together with calculated pyroxene Mg#s produced during fractional crystallization of a eucritic residual liquid from the equilibrium crystallization sequence (from 1250 to 1100 °C; open triangles; Table 4). The cumulate eucrite data are from Takeda and Mori (1985), Mittlefehldt and Lindstrom (1993), Pun and Papike (1995), Ishii and Takeda (1974), Duke and Silver (1967) and Lovering (1975).

physical scenario for production of the evolved Nuevo Laredo trend eucrites and cumulate eucrites during fractional crystallization of a residual Main Group eucrite liquid. Previous workers have noted several lines of evidence for a fractionation trend in eucrites with Nuevo Laredo representing a more fractionated melt (Stolper, 1977; Warren and Jerde, 1987). Using the MELTS program, the 1250 °C residual liquid composition (from the equilibrium crystallization sequence described in the previous section) has been cooled along a fractional crystallization path showing the evolution of the residual liquids (Table 4; Fig. 5). These trends closely match the range of evolved eucrites, especially with respect to the Al_2O_3, FeO and MgO contents (Fig. 5). The Mg# of pigeonite produced in such fractionation trends is plotted together with the Mg#s of pigeonite from the cumulate eucrites in Fig. 6. The striking overlap in both of these sequences, along with predicted high An-content plagioclase feldspars (~An_{86-84}; Table 4), confirms the idea that the cumulate eucrites represent cumulates from a fractionation sequence of a Main Group to evolved eucrite.

Previous studies (*e.g.*, Warren and Jerde, 1987) have demonstrated that a fractionation origin for the Nuevo Laredo trend eucrites is consistent with the incompatible trace element data. Although some studies have found that the liquids parental to the cumulate eucrites were LREE enriched and noneucritic (Pun and Papike, 1995), recent work has shown that when trapped intercumulus liquid is taken into account, the cumulate eucrites are readily related to eucritic parent liquids (Saiki and Takeda, 1994; Treiman, 1997). We will not treat this issue quantitatively but rather refer the reader to these previous studies.

Measurements of Pb isotopes in three noncumulate and three cumulate eucrites indicate a difference in the U/Pb ratio (μ) of these two classes of eucrite (μ = 14 for cumulate eucrites and 150 for noncumulate eucrites) and, thus, an origin on two separate planetesimals, or a single heterogeneous or layered parent body (Tera *et al.*, 1997). Some of the difference in μ values may be accounted for by the dominance of feldspar in the cumulate eucrites, since feldspar concentrates Pb over U and would, thus, result in a lower μ value. The young ages for the cumulate eucrites also would suggest that magmatism on the HED parent body lasted as long as 150 Ma after T_0. These results are in contrast to analyses of Cr isotopes in eucritic samples, which show that many cumulate and noncumulate eucrites and diogenites fall along an isochron that is consistent with early Mn/Cr fractionation in the HED parent body, ~3 Ma after T_0 (Lugmair and Shukolyukov, 1997; Shukolyukov and Lugmair, 1997). These two lines of research (Tera *et al.*, 1997; Shukolyukov and Lugmair, 1997) have made use of different subsets of eucrite samples, with the exception of Moore County, which is a cumulate eucrite yielding a

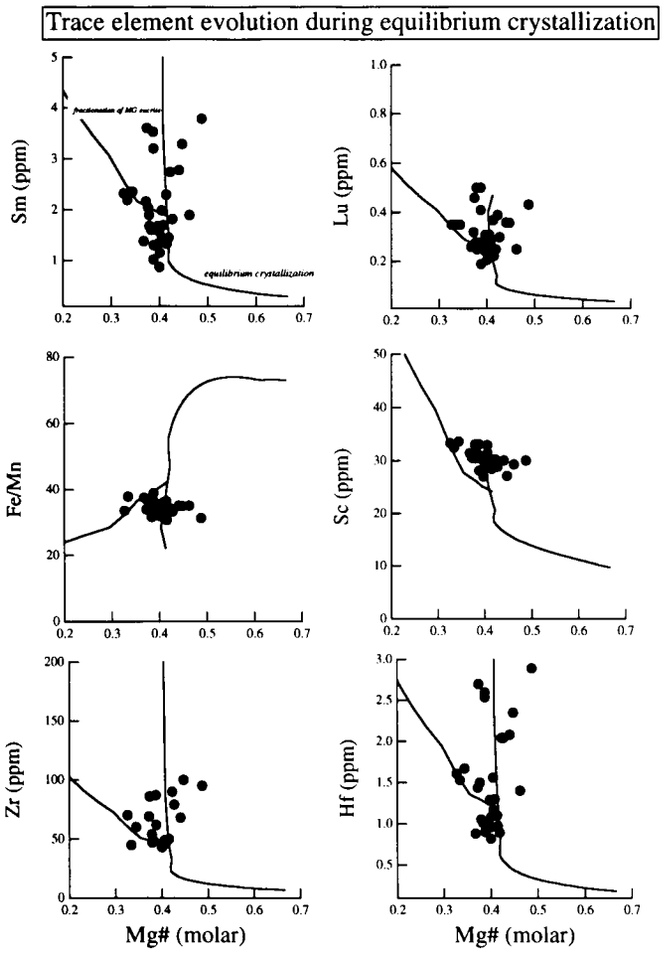

FIG. 8. Calculated trace element concentrations (for Sc, Zr, Lu, Sm, and Hf) and Fe/Mn *vs.* molar Mg# from calculated liquid compositions. Eucrite data are from BVSP, 1981, Fukuoka *et al.*, 1977; Palme *et al.*, 1978; Wänke *et al.*, 1972, 1974, 1977; Mittlefehldt, 1987; Warren and Jerde, 1987; Mittlefehldt and Lindstrom, 1993; Warren *et al.*, 1990; Morgan *et al.*, 1978; Palme and Ramensee, 1981; Schmitt *et al.*, 1964. Trace element concentrations are calculated using Eq. (13) in text, with partition coefficients (D) from Green (1994) and Horn *et al.* (1994). Manganese partition coefficients for olivine and orthopyroxene are from Watson (1977) and Colson *et al.* (1988), respectively. Calculated Mg#s are from MELTS calculations on the L-CV mix composition.

young age for both Pb (4.484 Ga) and Cr (<4.549 Ga) isotopic systems, and Serra de Magé, which is a cumulate eucrite yielding a younger Pb age (4.399 Ga) and an older Cr age (4.552 Ga). The different results for Serra de Magé suggest that the younger Pb age dates a secondary event. Perhaps with more Pb and Cr isotopic analyses, it will be necessary to consider multiple parent bodies for some of the cumulate and noncumulate eucrites; our modeling is ultimately applicable to single or multiple parent bodies, but we see no reason to absolutely exclude the possibility that most HED meteorites originated from a common body such as Vesta.

Step 4: Thermal History and Metamorphism and Later Ejection of Material from the Howardite, Eucrite, Diogenite Parent Body

The predicted crystallization sequence of *equilibrium* crystallization in a magma ocean followed by *fractional* crystallization in magma bodies intruded into or extruded onto the primitive crust will

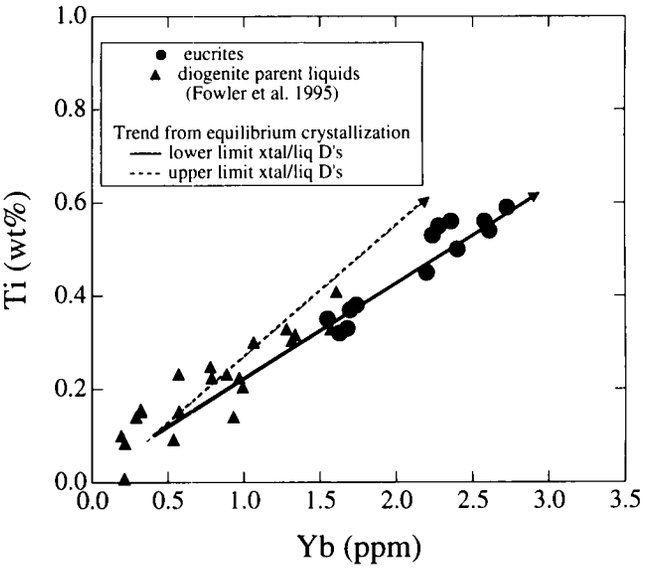

FIG. 9. Calculated Ti *vs.* Yb for equilibrium crystallization of magma ocean (Low-D and high-D calculations refer to two sets of calculations, those with values at the low and high ends of the range reported for each phase by Green (1994) and Horn *et al.* (1994)). Triangles are calculated parent magmas to diogenites (Fowler *et al.*, 1995). Solid circles are eucrites (reported by BVSP, 1981, Fukuoka *et al.*, 1977 and Palme *et al.*, 1978). The closer match between the "low-D" calculated trend and the diogenite parents/eucrites is consistent with the study of Colson *et al.* (1988), in which crystal/liquid partition coefficients are composition and temperature dependent; the lower Ds may be more appropriate for the higher temperature and more depolymerized melt of a magma ocean.

produce a layered mantle and crust. Estimates of the thicknesses of these layers for a Vesta size body may be made from the equilibrium crystallization calculations. Assuming a density of 3.4 g/cm^3 and a radius of 250 km (Schubart and Matson, 1979), the mass of Vesta would be 2.23×10^{23} g. A core of 10% of the mass of Vesta would have a radius of ~90 km, assuming a core density of 8.0 g/cm^3. At 23% crystallization of a L-CV chondrite magma ocean (cooling from 1620 °C to 1530 °C), olivine would be the sole liquidus phase; complete settling at this point would result in a dunitic layer to a radius of ~130 km (~40 km thick). After 80% equilibrium crystallization of the remaining liquid (magma ocean) 1530 °C to 1220 °C, olivine (25%), pyroxene (72%) and spinel (3%) would be present with 20% melt; complete segregation of melt from crystals at this point (highly likely from a convective point of view) would result in a solid mantle out to a radius of 240 km, with a 10–15 km thick outer layer of basaltic material.

Textures and exsolution lamellae in eucrites are consistent with such a thin basaltic crust. Two-pyroxene thermometry and textural observations of equilibrated eucrites indicate that eucrites were metamorphosed at conditions from 700 to 1000 °C, most likely due to burial in a thin crust (Yamaguchi *et al.*, 1996). Studies of the thickness of augite exsolution lamellae in the cumulate eucrite Moore County yield estimates of crustal thicknesses of ~8 km (Miyamoto and Takeda, 1994). Pyroxene crystallography and textures in polymict breccias, diogenites and eucrites are also consistent with a layered, thin (1–10 km) crust on the HED parent body (Takeda *et al.*, 1976; Takeda, 1979). In addition, spectral studies (Binzel and Xu, 1993) have identified chunks of eucritic material as large as 10 km.

Given these layering constraints, it is clear that impacts could easily excavate and penetrate the thin eucritic crust to expose dioge-

TABLE 4. Liquid compositions produced during fractional crystallization of a residual liquid (1250 °C) from the equilibrium crystallization sequence (1 bar and IW buffer).

T °C	SiO_2	TiO_2	Al_2O_3	Cr_2O_3	FeO	MgO	CaO	Na_2O	olivine Mg#	pyroxene Mg#	plagioclase X_{An}
1250	48.4	0.70	11.90	0.29	18.71	9.85	9.52	0.57	0.74	—	—
1240	48.4	0.71	12.00	0.29	18.68	9.61	9.60	0.57	0.73	—	—
1230	48.6	0.72	12.17	0.27	18.60	9.20	9.74	0.58	0.72	—	—
1220	48.8	0.73	12.35	0.26	18.51	8.79	9.88	0.59	0.71	—	—
1210	48.8	0.74	12.56	0.24	18.50	8.42	10.04	0.60	0.71	0.67	—
1200	48.7	0.76	12.83	0.23	18.53	8.01	10.23	0.62	—	0.65	—
1190	48.6	0.78	13.10	0.21	18.54	7.60	10.42	0.64	—	0.63	—
1180	48.5	0.80	13.38	0.20	18.55	7.19	10.60	0.65	—	0.61	—
1170	48.4	0.86	13.27	0.19	19.07	6.69	10.72	0.66	—	0.59	0.86
1160	48.3	0.99	12.54	0.20	20.43	6.07	10.73	0.64	—	0.56	0.86
1150	48.1	1.13	11.87	0.20	21.65	5.49	10.75	0.62	—	0.53	0.85
1140	48.0	1.27	11.27	0.20	22.78	4.92	10.78	0.60	—	0.50	0.85
1130	47.9	1.42	10.71	0.20	23.82	4.38	10.81	0.58	—	0.47	0.84
1120	47.8	1.57	10.21	0.20	24.76	3.86	10.84	0.57	—	0.43	0.84
1110	47.7	1.74	9.76	0.19	25.63	3.35	10.86	0.55	—	0.40	0.83

nitic material below, such as reported by Gaffey (1983). The ejection of kilometer size chunks of Vesta could be achieved by a 10–20 km size impactor, at a velocity of 8 km/s, without disrupting or destroying Vesta (Asphaug, 1996). Recent Hubble Space Telescope images of Vesta also show several areas that may be diogenitic rather than basaltic, and more detailed characterization of these features is of great interest with reference to the HED meteorite clan.

DISCUSSION

Comparison to Previous Models

There are two general classes of models for the origin of HED meteorites, both with problematic aspects. The first hypothesis is that the eucrites are the end result of a fractional crystallization sequence, the cumulates of which are represented by the diogenites and cumulate eucrites (*e.g.*, Mason, 1962; Ikeda and Takeda, 1985; Warren, 1985a; Delaney *et al.*, 1984; Bartels and Grove, 1991; Longhi and Pan, 1988). None of these models has been able to account for all of the compositional variation seen in either the liquids or the cumulates without appealing to several different melting or fractionation events, polybaric fractionation (Longhi and Pan, 1988), or localized heating within the mantle of the parent body (*e.g.*, Grove and Bartels, 1992). The recent models of Ruzicka *et al.* (1996, 1997) are examples of models with both physical and compositional problems. For example, pure fractional crystallization of a magma ocean will be unlikely given the enhanced conditions (low gravity, parallel adiabat and solidus/liquidus slopes) for entrainment on an asteroid size body, and the production of diogenite deep within (~100 km) the HED parent body makes them difficult to deliver through impact processes with complete disruption of the parent body. Also, their choice of a source material that is 2.5 to 3× chondritic in the refractory elements seems arbitrary; despite this choice, the calculated residual liquids are not eucritic in detail (see Fig. 4).

The second hypothesis argues that eucrites are the result of equilibrium partial melting of primitive chondritic material (*e.g.*, Stolper, 1977; Consolmagno and Drake, 1977). Although the partial melting hypothesis is consistent with the clustering of the eucrites around the olivine-pyroxene peritectic point on an olivine-pyroxene-plagioclase phase diagram, and can explain much of the compositional data (see summary within Stolper, 1977), it fails to account for the diogenites in a simple petrogenetic model (Shearer *et al.*, 1993; Mittlefehldt, 1994) and for the low Na contents of the eucritic plagioclase and HED parent body (Mason, 1969). Core formation also presents a problem, as siderophile element abundances indicate that the core formed prior to the production of eucrites as the eucrite source was demonstrably metal-free (Fig. 2). Core formation requires substantial melting of the silicates to facilitate metal segregation. Multiple heating events required to allow core separation from a substantially molten body, followed by solidification and subsequent partial melting to produce both the broad range of eucrite melts (low, moderate and high degree melting) as well as later remelting of the residual mantle to produce the diogenites are unlikely. Finally, the primitive unmelted material required in these models has not been identified in the meteorite collections (other than rare ultramafic clasts such as those described by Smith and Schmitt, 1982 from the Kapoeta howardite).

The magma ocean model presented here provides several advantages over previous fractional crystallization and partial melting models. First, it requires one single melting event to provide a mostly molten silicate mantle for core separation; later crystallization of that mantle can produce the range of cumulate and noncumulate igneous lithologies represented in the HED meteorite collections. Second, it obviates the need for unmelted primitive material that is required of partial melting models; the high temperature during core formation leaves olivine (and perhaps a thin outer conductive boundary layer) as the sole surviving silicate material and it most likely sinks into a dunitic layer. Third, it provides a way of having both eucrites and diogenites at relatively shallow depths on the same parent body. Fourth, it explains why we do not see the magnesian parent liquids for diogenites; they have since crystallized further to form more cumulates and residual eucritic liquids. And fifth, the bulk composition is known material that satisfies a broad range of cosmochemical data such as major elements, O isotopes, Fe/Mn, Mn/Cr and Hf/W ratios, and siderophile and incompatible element concentrations.

Implications for Volatile Elements Depletions

Despite the ability of this model to account for so many compositional features in the eucrites and diogenites, there is no way to reconcile the low Na and K abundances of the eucrites with a chondritic bulk composition. The Na_2O content required to form eucrites from the L-CV mantle composition presented here is 0.1 wt%, which is ~10× lower than that measured in chondrites. This alkali problem was recognized as early as Gast (1960) and Mason (1969) and is evident also in the chondrite melting experiments of Jurewicz *et al.* (1995) in that they did not crystallize An-rich plagioclase (as observed in the eucrites). In fact, crystallization calculations for compositions with a full complement of chondritic Na and K result in andesitic liquids (58 to 60% SiO_2 and 4 to 8% alkalis) that have a large olivine stability field. These are quite different from eucritic liquids both in bulk composition and the nature of the saturated phases. Recent measurements of K isotopes indicate that a broad range of solar system materials (chondrites, achondrites) shows no evidence for fractionation that might be expected if these volatile elements were depleted during Rayleigh fractionation or a magmatic volatile loss event (Humayun and Clayton, 1996). This suggests that

these elements were perhaps only partially condensed (Humayun and Clayton, 1996) in an early, hot solar nebula (*e.g.* Boss, 1993). What is clear is that material of volatile-depleted chondritic composition can be building blocks for the HED parent body rather than unusual and odd nonchondritic materials.

CONCLUSIONS

Our result indicates that the eucrites and diogenites may have formed during crystallization of an extensive magma ocean, thus requiring only one initial heat source in the early solar system. This simple physicochemical model for the origin of the howardite, eucrite and diogenite meteorites has the following highlights.

(1) An early magma ocean fostered rapid and high-temperature metal-silicate equilibrium between a small core and molten mantle (Fig. 10a).

(2) *Equilibrium* crystallization of the roughly chondritic molten mantle ensued (Fig. 10b), with crystals of olivine, orthopyroxene and spinel suspended in the magma ocean until ~0.80 crystal fraction (Fig. 10c). At this point, the viscous solid-liquid mush convected at such a slow rate that it could not avoid gravitational segregation of magma from solid silicates.

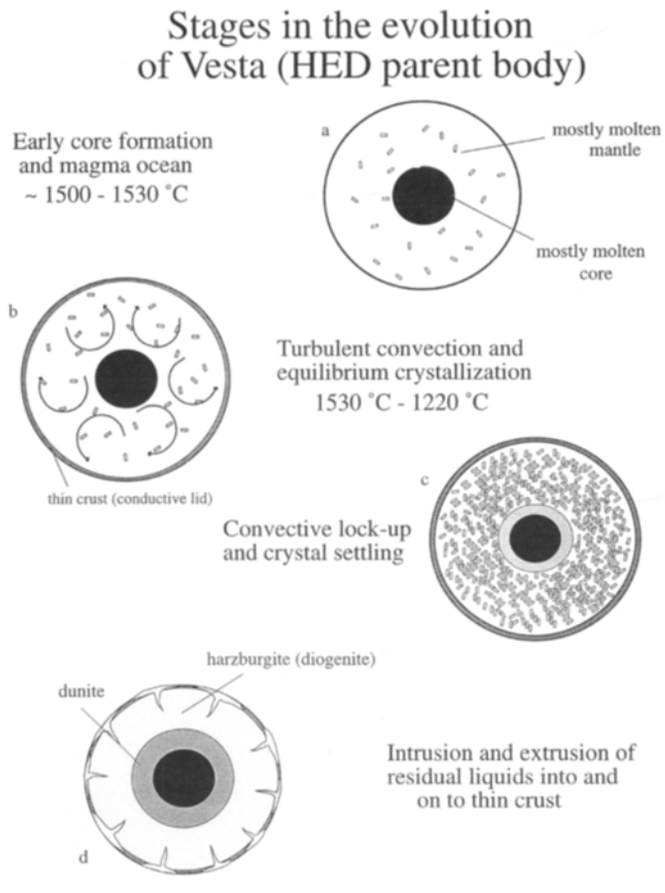

FIG. 10. Schematic diagram showing stages in the cooling and crystallization history of a Vesta size eucrite/diogenite parent body. (a) Global magma ocean fosters efficient metal-silicate separation; mantle abundances of siderophile elements set by high-temperature metal-silicate equilibrium. (b) Equilibrium crystallization and convection of magma ocean until ~0.20 mass fraction liquid; note thin outer crust (conductive lid). (c) Ocean becomes too viscous and convection halts; gravitational segregation ensues. (d) residual liquid (Main Group eucrites) is forced out to surface and crystals accumulate at depth (dunites deep and diogenites shallow) in asteroid. Some eucritic liquid is isolated in magma chambers to produce evolved basalt (Nuevo Laredo fractionation trend). Later impacts can penetrate the basaltic crust to depths of the uppermost diogenites (lowest Mg# in Fig. 7). Additional brecciation and gardening of the surface materials will produce howardites.

(3) Residual liquids (Main Group eucrites) were extruded onto the surface and/or into a primitive crust, with the uppermost set of crystalline cumulates forming diogenites (Fig. 10d). *Fractionation* of bodies of this eucritic liquid within the thin outer crust produced the evolved (Nuevo Laredo trend) eucrites at the same time as the cumulate eucrites (Fig. 10d).

(4) Complete crystallization occurred within 20 Ma after T_0, (the age of refractory inclusions in the Allende CV3 chondrite; Allegre *et al.*, 1995) thus obviating the need for anomalous, high T events either deep within or just below the surface of the HED parent body.

(5) Later impacts and cratering produced the material that has since been delivered to Earth in the form of the HED meteorites. The penetration depths of at least 15 km are consistent with sampling of both eucritic materials (both cumulate and noncumulate) and the uppermost cumulate layers of diogenites, and physical modeling of kilometer size impactors.

Acknowledgments–This work was stimulated by the LPI-sponsored HED/Vesta Workshop in October 1996. This manuscript benefitted from the thoughtful and critical reviews of D. M. Shaw, C. K. Shearer and H. Takeda. This research is supported through NASA Grants NAGW-3348 and NAG5-4084.

Editorial handling: D. M. Shaw

REFERENCES

ABE Y. (1992) Thermal evolution and chemical differentiation of the terrestrial magma ocean. In *Evolution of the Earth and Planets* (eds. R. Jeanloz and D. Weidner), pp. 41–54. *Geophys Monogr.* **74**, IUGG Vol. 14, IUGG/AGU, Washington, D.C.

AGEE C. B., LI J., SHANNON M. C. AND CIRCONE S. (1995) Pressure-temperature diagram for the Allende meteorite. *J. Geophys. Res.* **100**, 17 725–17 740.

ALLEGRE C. J., MANHES G. AND GOPEL C. (1995) The age of the Earth. *Geochim. Cosmochim. Acta* **59**, 1445–1456.

ARNDT N. T. (1986) Differentiation of komatiite flows. *J. Petrol.* **27**, 279–301.

ASPHAUG E. (1996) *Large Ejecta Fragments from Vesta and Other Asteroids*. LPI Tech. Rept. **96**–02. 44 pp.

BARTELS K. S. AND GROVE T. L. (1991) High-pressure experiments on magnesian eucrite compositions: Constraints on magmatic processes in the eucrite parent body. *Proc. Lunar Planet. Sci. Conf.* **21st**, 351–365.

BASALTIC VOLCANISM STUDY PROJECT (BVSP) (1981) *Basaltic Volcanism on the Terrestrial Planets*. Pergamon Press, New York, New York. 1286 pp.

BINZEL R. P. AND XU S. (1993) Chips off of asteroid 4 Vesta: Evidence for the parent body of basaltic achondrite meteorites. *Science* **260**, 186–191.

BOESENBERG J. S. AND DELANEY J. S. (1997) A model composition of the basaltic achondrite planetoid. *Geochim. Cosmochim. Acta* **61**, 3205–3226.

BOSS A. P. (1993) Evolution of the solar nebula. II. Thermal structure during nebula formation. *Astrophys. J.* **417**, 351–367.

BOTTINGA Y. AND WEILL D. F. (1972) The viscosity of magmatic silicate liquids: A model for calculation. *Am. J. Sci.* **272**, 438–475.

BUCHANAN P. C. AND REID A. R. (1996) Petrology of the polymict eucrite Petersburg. *Geochim. Cosmochim. Acta* **60**, 135–146.

BUCHWALD V. F. (1977) *Handbook of Iron Meteorites: Volume 1*. University of California Press, Los Angeles, California. 242 pp.

CAPOBIANCO C. J., JONES J. H. AND DRAKE M. J. (1993) Metal-silicate thermochemistry at high temperature: Magma oceans and the "excess siderophile element" problem of the Earth's Upper Mantle. *J. Geophys. Res.* **98**, 5433–5443.

CARLSON R. W., TERA F. AND BOCTOR N. Z. (1988) Radiometric geochronology of the eucrites Nuevo Laredo and Bereba (abstract). *Lunar Planet. Sci.* **19**, 166–167.

CHEN C-Y., FREY F. A., GARCIA M. O., DALRYMPLE G. B. AND HART S. R. (1991) The tholeiite to alkalic basalt transition at Haleakala Volcano, Maui, Hawaii. *Contrib. Mineral. Petrol.* **106**, 183–200.

CLAYTON R. N. AND MAYEDA T. K. (1996) Oxygen isotopes studies of achondrites. *Geochim. Cosmochim. Acta* **60**, 1999–2017.

COLSON R. O., MCKAY G. A. AND TAYLOR L. A. (1988) Temperature and composition dependencies of trace element partitioning: Olivine/melt and low-Ca pyroxene/melt. *Geochim. Cosmochim. Acta* **52**, 539–553.

CONSOLMAGNO G. J. AND DRAKE M. J. (1977) Composition and evolution of the eucrite parent body: Evidence from rare earth elements. *Geochim. Cosmochim. Acta* **41**, 1271–1282.

CRAWFORD A. J. AND CAMERON W. E. (1985) Petrology and geochemistry of Cambrian boninites and low-Ti andesites from Heathcote, Victoria. *Contrib. Mineral. Petrol.* **91**, 93–104.

DELANEY J. S., PRINZ M. AND TAKEDA H. (1984) The polymict eucrites. *Proc. Lunar Planet. Sci. Conf.* **15th**, C251–C288.

DELANO J. W. (1986) Abundances of cobalt, nickel, and volatiles in the silicate portion of the Moon. In *Origin of the Moon* (eds. W. K. Hartmann, R. J. Phillips and G. J. Taylor), pp. 231–248. Lunar and Planetary Institute, Houston, Texas.

DICKEY J. S., FREY F. A., HART S. R., WATSON E. B. AND THOMPSON G. (1977) Geochemistry and petrology of dredged basalts from the Bouvet triple junction, South Atlantic. *Geochim. Cosmochim. Acta* **41**, 1105–1118.

DRAKE M. J., NEWSOM H. E. AND CAPOBIANCO C. J. (1989) V, Cr, and Mn in the Earth, Moon, EPB and SPB and the origin of the Moon: Experimental studies. *Geochim. Cosmochim. Acta* **53**, 2101–2111.

DREIBUS G. AND WÄNKE H. (1980) The bulk composition of the eucrite parent asteroid and its bearing on planetary evolution. *Z. Naturforsch.* **35a**, 204–216.

DREIBUS G., PALME H., SPETTEL B., ZIPFEL J. AND WÄNKE H. (1995) Sulfur and selenium in chondritic meteorites. *Meteoritics* **30**, 439–445.

DUKE M. B. AND SILVER L. T. (1967) Petrology of eucrites, howardites and mesosiderites. *Geochim. Cosmochim. Acta* **31**, 1637–1665.

FOWLER G. W., PAPIKE J. J., SPILDE M. N. AND SHEARER C. K. (1994) Diogenites as asteroidal cumulates: Insights from orthopyroxene major and minor element chemistry. *Geochim. Cosmochim. Acta* **58**, 3921–3929.

FOWLER G. W., SHEARER C. K., PAPIKE J. J. AND LAYNE G. D. (1995) Diogenites as asteroidal cumulates: Insights from orthopyroxene trace element chemistry. *Geochim. Cosmochim. Acta* **59**, 3071–3084.

FUKUOKA T., BOYNTON W. V., MA M-S. AND SCHMITT R. A. (1977) Genesis of howardites, diogenites and eucrites. *Proc. Lunar Planet. Sci. Conf.* **8th**, 187–210.

GAFFEY M. J. (1983) The asteroid (4) Vesta: Rotational spectral variations, surface material heterogeneity, and implications for the origin of the basaltic achondrites (abstract). *Lunar Planet. Sci.* **14**, 231–232.

GAST P. W. (1960) Alkali metals in stone meteorites. *Geochim. Cosmochim. Acta* **19**, 1–4.

GHIORSO M. S. AND SACK R. O. (1995) Chemical mass transfer in magmatic processes IV. A revised and internally consistent thermodynamic model for the interpolation and extrapolation of liquid-solid equilibria in magmatic systems at elevated temperatures and pressures. *Contrib. Mineral. Petrol.* **119**, 197–212.

GHOSH A. AND MCSWEEN H. Y., JR. (1996) *The Thermal History of Asteroid 4 Vesta, Based on Radionuclide and Collisional Heating.* LPI Tech. Rept. **96–02**, 9–10.

GREEN T. H. (1994) Experimental studies of trace element partitioning applicable to igneous petrogenesis—Sedona 16 years later. *Chem. Geol.* **117**, 1–36.

GROVE T. L. AND BARTELS K. S. (1992) The relation between diogenite cumulates and eucrite magmas. *Proc. Lunar Planet. Sci. Conf.* **22nd**, 437–445.

HARPER C. L. AND JACOBSEN S. B. (1995) Accretion and differentiation history of the Earth based on extinct radionuclides. In *Isotopic Studies of Crust-Mantle Evolution* (eds. A. R. Basu and S. R. Hart), pp. 47–74. American Geophysical Union, San Francisco, California.

HEWINS R. H. (1981) Orthopyroxene-olivine assemblages in diogenites and mesosiderites. *Geochim. Cosmochim. Acta* **45**, 123–126.

HEWINS R. H. AND NEWSOM H. E. (1988) Igneous activity in the early solar system. In *Meteorites and the Early Solar System* (eds. J. F. Kerridge and M. S. Matthews.), pp. 73–101. University of Arizona Press, Tucson, Arizona.

HORN I., FOLEY S. F., JACKSON S. E. AND JENNER G. A. (1994) Experimentally determined partitioning of high field strength- and selected transition elements between spinel and basaltic melt. *Chem. Geol.* **117**, 193–218.

HUMAYUN M. AND CLAYTON R. N. (1995) Potassium isotope cosmochemistry: Genetic implications of volatile element depletion. *Geochim. Cosmochim. Acta* **59**, 2131–2148.

IKEDA Y. AND TAKEDA H. (1985) A model for the origin of basaltic achondrites based on the Yamato 7308 howardite. *Proc. Lunar Planet. Sci Conf.* **15th**; *J. Geophys. Res.* **90 (Suppl.)**, C649–C663.

ISHII T. AND TAKEDA H. (1974) Inversion, decomposition and exsolution phenomena of terrestrial and extraterrestrial pigeonites. *Mem. Geol. Soc. Japan* **11**, 19–36.

JAGOUTZ E., PALME H., BADDENHAUSEN H., BLUM K., CENDALES M., DREIBUS G., SPETTEL B., LORENZ V. AND WÄNKE H. (1979) The abundances of major, minor and trace elements in the earth's mantle as derived from primitive ultramafic nodules. *Proc. Lunar Planet. Sci. Conf.* **10th**, 2031–2050.

JOCHUM K. P., MCDONOUGH W. F., PALME H. AND SPETTEL B. (1989) Compositional constraints on the continental lithospheric mantle from trace elements in spinel peridotite xenoliths. *Nature* **340**, 548–550.

JONES J. H. (1984) The composition of the mantle of the eucrite parent body and the origin of eucrites. *Geochim. Cosmochim. Acta* **48**, 641–648.

JONES J. H., MITTLEFEHLDT D. W., JUREWICZ A. J. G., LAUER H. V., JR., HANSON B. Z., PASLICK C. R. AND MCKAY G. A. (1996) *The Origin of Eucrites: An Experimental Perspective.* LPI Tech. Rept. **96–02**, 15.

JUREWICZ A. J. G., MITTLEFEHLDT D. W. AND JONES J. H. (1991) Partial melting of the Allende (CV3) meteorite: Implications for origins of basaltic meteorites. *Science* **252**, 695–698.

JUREWICZ A. J. G., MITTLEFEHLDT D. W. AND JONES J. H. (1995) Experimental partial melting of the St. Severin (LL) and Lost City (H) chondrites. *Geochim. Cosmochim. Acta* **59**, 391–408.

KAY R., HUBBARD N. J. AND GAST P. W. (1970) Chemical characteristics and origin of oceanic ridge volcanic rocks. *J. Geophys. Res.* **75**, 1585–1613.

KRAICHAN R. H. (1962) Turbulent thermal convection at arbitrary Prandtl number. *Phys. Fluids* **5**, 1374–1389.

KRESS V. C. AND CARMICHAEL I. S. E. (1991) The compressibility of silicate liquids containing Fe_2O_3 and the effect of composition, temperature, oxygen fugacity and pressure on their redox states. *Contrib. Mineral. Petrol.* **108**, 82–92.

KUBASCHEWSKI O. (1982) *Iron Binary Phase Diagrams.* Springer-Verlag, Berlin, Germany. 179 pp.

LANGE R. A. AND CARMICHAEL I. S. E. (1987) Densities of Na_2O-K_2O-CaO-MgO-FeO-Fe_2O_3-Al_2O_3-TiO_2-SiO_2 liquids: New measurements and derived partial molar properties. *Geochim. Cosmochim. Acta* **53**, 2195–2204.

LEE D-C. AND HALLIDAY A. N. (1996) Hafnium-tungsten chronometry and the timing of terrestrial core formation. *Nature* **378**, 771–774.

LEE D-C. AND HALLIDAY A. N. (1997) Hf-W evidence for early differentiation of Mars and the eucrite parent body (abstract). *Lunar Planet. Sci.* **28**, 795–796.

LONGHI J. (1987) On the connection between mare basalts and picritic volcanic glasses. *Proc. Lunar Planet. Sci. Conf.* **17th**, E349–E360.

LONGHI J. AND PAN V. (1988) Phase equilibrium constraints on the howardite-eucrite-diogenite association. *Proc. Lunar Planet. Sci. Conf.* **18th**, 459–470.

LOVERING J. F. (1975) The Moama eucrite–A pyroxene-plagioclase adcumulate. *Meteoritics* **10**, 101–114.

LUGMAIR G. W. AND SHULOLYUKOV A. (1997) ^{53}Mn-^{53}Cr isotope systematics of the HED parent body (abstract). *Lunar Planet. Sci.* **28**, 851–852.

MARSH B. D. (1988) Crystal capture, sorting, and retention in convecting magma. *Geol. Soc. Amer. Bull.* **100**, 1720–1737.

MARTIN D. AND NOKES R. (1988) Crystal settling in a vigorously convecting magma chamber. *Nature* **332**, 534–536.

MASON B. (1962) *Meteorites.* John Wiley and Sons, New York, New York. 274 pp.

MASON B. (1969) The Bununu meteorite, and a discussion of the pyroxene plagioclase achondrites. *Geochim. Cosmochim. Acta* **31**, 107–115.

MCCORD T. B., ADAMS J. B. AND JOHNSON T. V. (1970) Asteroid Vesta: Spectral reflectivity and compositional implications. *Science* **168**, 1445–1447.

MCKENZIE D. AND BICKLE M. J. (1988) The volume and composition of melt generated by extension of the lithosphere. *J. Petrol.* **29**, 625–679.

MITTLEFEHLDT D. W. (1979) Petrographic and chemical characterization of igneous lithic clasts from mesosiderites and howardites and comparison with eucrites and diogenites. *Geochim. Cosmochim Acta* **43**, 1917–1935.

MITTLEFEHLDT D. W. (1987) Volatile degassing of basaltic achondrite parent bodies: Evidence from alkali elements and phosphorus. *Geochim. Cosmochim Acta* **51**, 267–278.

MITTLEFEHLDT D. W. (1994) The genesis of diogenites and HED parent body petrogenesis. *Geochim. Cosmochim Acta* **58**, 1537–1552.

MITTLEFEHLDT D. W. AND LINDSTROM M. M. (1993) Geochemistry and petrology of a suite of ten Yamato HED meteorites. *Proc. NIPR Symp. Antarct. Meteorites* **6**, 268–292.

MITTLEFEHLDT D. W. AND LINDSTROM M. M. (1997) Magnesian basalt clasts from the EET 92014 and Kapoeta howardites and a discussion of alleged primary magnesian HED basalts. *Geochim. Cosmochim Acta* **61**, 453–462.

MIYAMOTO M. (1991) Significance of ^{26}Al as heat source of meteorite parent bodies. *Proc. ISAS Lunar and Planet. Symp.* **24th**, *Inst. Space Aeron. Sci.*, 248–254.

MIYAMOTO M. AND TAKEDA H. (1994) Evidence for excavation of deep crustal material of a Vesta-like body from Ca compositional gradients

in pyroxene. *Earth Planet. Sci Lett.* **122**, 343–349.
MORGAN J. W., HIGUCHI H., TAKAHASHI H. AND HERTOGEN J. (1978) A "chondritic" eucrite parent body: Inference from trace elements. *Geochim. Cosmochim Acta* **42**, 27–38.
MURASE T. AND MCBIRNEY A. R. (1973) Properties of some common igneous rocks and their melts at high temperatures. *Geol. Soc. Amer. Bull.* **84**, 3563–3592.
NEWSOM H. E. (1985) Molybdenum in eucrites: Evidence for a metal core in the eucrite parent body. *J. Geophys. Res.* **90 (Suppl.)**, C613–C617.
NEWSOM H. E. (1995) Composition of the solar system, planets, meteorites, and major terrestrial reservoirs. In *Global Earth Physics: A Handbook of Physical Constants: AGU Reference Shelf volume 1* (ed. T. J. Ahrens), pp. 159–189. American Geophysical Union, Washington, D.C.
NEWSOM H. E. AND DRAKE M. J. (1982) The metal content of the eucrite parent body: Constraints from the partitioning behavior of tungsten. *Geochim. Cosmochim Acta* **46**, 2483–2489.
NEWSOM H. E., SIMS K. W. W., NOLL P. D., JR., JAEGER W. L., MAEHR S. A. AND BESERRA T. B. (1996) The depletion of tungsten in the bulk silicate earth: Constraints on core formation. *Geochim. Cosmochim. Acta* **60**, 1155–1169.
NYQUIST L. E., TAKEDA H., BANSAL B. M., SHIH C-Y., WIESMANN H. AND WOODEN J. L. (1986) Rb-Sr and Sm-Nd internal isochron ages of a subophitic basalt clast and a matrix sample from the Y75011 eucrite. *J. Geophys. Res.* **91**, 8137–8150.
PALME H. AND RAMMENSEE W. (1981) The significance of W in planetary differentiation processes: Evidence from new data on eucrites. *Proc. Lunar. Planet. Sci. Conf.* **12B**, 949–964.
PALME H., BADDENHAUSEN H., BLUM K., CENDALES M., DREIBUS G., HOFMEISTER H., KRUSE H., PALME C., SPETTEL B., VILCZEK E., WÄNKE H. AND KURAT G. (1978) New data on lunar samples and achondrites and a comparison of the least fractionated samples from the Earth, Moon and the eucrite parent body. *Proc. Lunar Planet. Sci. Conf.* **9th**, 25–57.
PUN A. AND PAPIKE J. J. (1995) Ion microprobe investigation of exsolved pyroxenes in cumulate eucrites: Determination of selected trace element partition coefficients. *Geochim. Cosmochim Acta* **59**, 2279–2289.
RIGHTER K. AND DRAKE M. J. (1996) Core formation in Earth's Moon, Mars and Vesta. *Icarus* **124**, 513–529.
RIGHTER K., DRAKE M. J. AND YAXLEY G. (1997) Prediction of siderophile element metal-silicate partition coefficients to 120 kb and 2800 °C: The effect of pressure, temperature, fO_2 and melt composition. *Phys. Earth Planet. Int.* **100**, 115–134.
RUSSELL S. S., SRINIVASAN G., HUSS G. R., WASSERBURG G. J. AND MACPHERSON G. J. (1996) Evidence for widespread ^{26}Al in the solar nebula and constraints for nebula time scales. *Science* **273**, 757–762.
RUZICKA A., SNYDER G. A. AND TAYLOR L. A. (1996) *Asteroid 4 Vesta as the HED Parent Body: Implications for a Metallic Core and Magma Ocean Crystallization.* LPI Tech. Rept. **96–02**, 23–24.
RUZICKA A., SNYDER G. A. AND TAYLOR L. A. (1997) Formation of eucrites and diogenites in a magma ocean on the HED parent body (abstract). *Lunar Planet. Sci.* **28**, 1215–1216.
SACK R. O., AZEREDO W. J. AND LIPSCHUTZ M. E. (1991) Olivine diogenites: The mantle of the eucrite parent body. *Geochim. Cosmochim. Acta* **55**, 1111–1120.
SAIKI K. AND TAKEDA H. (1994) The origin of cumulate eucrite deduced from magma differentiation simulation. *Proc. NIPR Symp. Antarct. Meteorites* **7**, 47–50.
SCHMITT R. A., SMITH R. H. AND OLEHY D. A. (1964) Rare earth, yttrium and scandium abundances in meteorite and terrestrial matter-II. *Geochim. Cosmochim. Acta* **28**, 67–86.
SCHUBART J. AND MATSON D. L. (1979) Masses and densities of asteroids. In *Asteroids* (ed. T. Gehrels), pp. 84–97. University of Arizona Press, Tucson, Arizona.
SCHWANDT C. S. AND MCKAY G. A. (1996) *REE Partition Coefficients from Synthetic Diogenite-like Enstatite and the Implications of Petrogenetic Modelling.* LPI Tech. Rept. **96–02**, 25–26. 44 pp.
SHEARER C. K., PAPIKE J. J. AND LAYNE G. D. (1993) Orthopyoxenes as recorders of diogenite petrogenesis: Trace element systematics (abstract). *Lunar Planet. Sci.* **24**, 1289–1290.
SHEARER C. K., FOWLER G. AND PAPIKE J. J. (1996) *Petrogenetic Models for the Origin of Diogenites and Their Relationship to Basaltic Magmatism on the HED Parent Body.* LPI Tech. Rept. **96–02**, 28–29.
SHUKOLYUKOV A. AND LUGMAIR G. W. (1993) Live Iron-60 in the early solar system. *Science* **259**, 1138–1143.
SHUKOLYUKOV A. AND LUGMAIR G. W. (1997) ^{53}Mn-^{53}Cr chronology of non-cumulate and cumulate eucrites (abstract). *Meteorit. Planet. Sci.* **32 (Suppl.)**, A120–A121.
SIMS K. W. W., NEWSOM H. E. AND GLADNEY E. S. (1990) Abundances of As, Sb, Mo, and W in the crust and mantle: Implications for terrestrial accretion and core formation through geologic time. In *The Origin of the Earth* (eds. H. E. Newsom and J. H. Jones), pp. 291–317. Oxford Press, London, U.K.
SMITH M. R. AND SCHMITT R. A. (1982) Chemical composition of the howardite parent body deduced from Kapoeta primary "mafic" magmas. *Proc. Lunar Planet. Sci Conf.* **13th**, A331–A338.
SNYDER D. A., GIER E. AND CARMICHAEL I. S. E. (1994) Experimental determination of the thermal conductivity of molten $CaMgSi_2O_6$ and the transport of heat through magmas. *J. Geophys. Res.* **99**, 15 503–15 516.
SPERA F. J. (1992) Lunar magma transport phenomena. *Geochim. Cosmochim. Acta* **56**, 2253–2266.
STOLPER E. M. (1977) Experimental petrology of eucritic meteorites. *Geochim. Cosmochim. Acta* **41**, 587–611.
TAKAHASHI E. (1983) Melting of a Yamato L3 chondrite (Y–74191) up to 30 kbar. *Mem. Natl. Inst. Polar Res., Spec. Issue* **30**, 168–180.
TAKEDA H. (1979) A layered crust model of a howardite parent body. *Icarus* **40**, 455–470.
TAKEDA H. (1986) Mineralogy of Yamato 791073 with reference to crystal fractionation of the howardite parent body. *Proc. Lunar Planet. Sci Conf.* **16th**, D355–D363.
TAKEDA H. AND MORI H. (1985) The diogenite-eucrite links and the crystallization history of a crust of their parent body. *Proc. Lunar Planet. Sci Conf.* **15th**; *J. Geophys. Res.* **90 (Suppl.)**, C636–C648.
TAKEDA H., MIYAMOTO M., ISHII T. AND REID A. M. (1976) Characterization of crust formation on a parent body of achondrites and the moon by pyroxene crystallography and chemistry. *Proc. Lunar Planet. Sci Conf.* **7th**, 3535–3548.
TAYLOR G. J. (1992) Core formation in asteroids. *J. Geophys. Res.* **97**, 14 717–14 726.
TAYLOR G. J., KEIL K., MCCOY T., HAACK H. AND SCOTT E. R. D. (1993) Asteroid differentiation: Pyroclastic volcanism to magma oceans. *Meteoritics* **28**, 34–52.
TERA F., CARLSON R. W. AND BOCTOR N. Z. (1997) Radiometric ages of basaltic achondrites and their relation to the early history of the Solar System. *Geochim. Cosmochim. Acta* **61**, 1713–1721.
TONKS W. B. AND MELOSH H. J. (1990) The physics of crystal settling and suspension in a turbulent magma ocean. In *Origin of the Earth* (eds. H. E. Newsom and J. H. Jones), pp. 151–174. Oxford Univ. Press, New York, New York.
TREIMAN A. H. (1997) The parent magma of the cumulate eucrites: A mass balance approach. *Meteorit. Planet. Sci.* **32**, 217–230.
WÄNKE H., BADDENHAUSEN H., BALACESCU A., TESCHKE F. SPETTEL B., DREIBUS G., PALME H., QUIJANO-RICO M., KRUSE H., WLOTZKA F. AND BEGEMANN F. (1972) Multi-element analyses of lunar samples and some implications of the results. *Proc. Lunar Sci. Conf.* **3rd**, 1251–1268.
WÄNKE H., PALME H., BADDENHAUSEN H., DREIBUS G., JAGOUTZ E., KRUSE H., SPETTEL B., TESCHKE F. AND THACKER R. (1974) Chemistry of Apollo 16 and 17 samples: Bulk composition, late stage accumulation and early differentiation of the Moon. *Proc. Lunar Sci. Conf.* **5th**, 1307–1335.
WÄNKE H., BADDENHAUSEN H., BLUM K., CENDALES M., DREIBUS G., HOFMEISTER H., KRUSE H., JAGOUTZ E., PALME C., SPETTEL B., THACKER R. AND VILCZEK E. (1977) On the chemistry of lunar samples and achondrites. *Proc. Lunar Planet. Sci. Conf.* **8th**, 2191–2213.
WARREN P. H. (1985a) Origin of howardites, diogenites and eucrites: A mass balance constraint. *Geochim. Cosmochim. Acta* **49**, 577–586.
WARREN P. H. (1985b) The magma ocean concept and lunar evolution. *Ann. Rev. Earth Planet. Sci.* **13**, 201–240.
WARREN P. H. AND JERDE E. A. (1987) Composition and origin of Nuevo Laredo trend eucrites. *Geochim. Cosmochim. Acta* **51**, 713–725.
WARREN P. H., JERDE E. A., MIGDISOVA L. F. AND YAROSHEVSKY A. A. (1990) Pomozdino: An anomalous, high MgO/FeO, yet REE-rich eucrite. *Proc. Lunar Planet. Sci. Conf.* **20th**, 281–297.
WARREN P. H., KALLEMEYN G. W., ARAI T. AND KANEDA K. (1996) Compositional-petrologic investigations of eucrites and the QUE 94201 shergottite. *Antarc. Meteor.* **21**, 195–197.
WATSON E. B. (1977) Partitioning of manganese between forsterite and silicate liquid. *Geochim. Cosmochim. Acta* **41**, 1363–1374.
WHITFORD D. J. AND ARNDT N. T. (1978) Rare earth element abundances in a thick, layered komatiite lava flow from Ontario, Canada. *Earth Planet. Sci Lett.* **41**, 188–196.
WILSON L. AND KEIL K. (1996) Volcanic eruptions and intrusions on the asteroid 4 Vesta. *J. Geophys. Res.* **101**, 18 927–18 940.
YAMAGUCHI A., TAYLOR G. J. AND KEIL K. (1996) Global crustal metamorphism of the Eucrite Parent Body. *Icarus* **124**, 97–112.